AALBORG UNIVERSITY

Composition to Structure

Statistical Mechanics for Glass Modeling

Bødker, Mikkel Sandfeld

Publication date:
2021

Document Version
Publisher's PDF, also known as Version of record

[Link to publication from Aalborg University]

COMPOSITION TO STRUCTURE: STATISTICAL MECHANICS FOR GLASS MODELING

BY
MIKKEL L. BØDKER

DISSERTATION SUBMITTED 2021

AALBORG UNIVERSITY
DENMARK

COMPOSITION TO STRUCTURE: STATISTICAL MECHANICS FOR GLASS MODELING

A PHD THESIS

by

Mikkel L. Bødker

AALBORG UNIVERSITY
DENMARK

Dissertation submitted 2021

ENGLISH SUMMARY

Oxide glasses are extensively researched, but the number of possible glass compositions is enormous because of the amorphous nature of the glassy structure. Data-based models accelerate the design of new oxide glasses with tailored properties by establishing composition-property relations. These composition-property models are often limited in their prediction to a limited compositional space similar to the training data because of the complex composition-property relation. Short-range order (SRO) structure-property models better predict properties in unknown glass compositions, but the amount of structure data available is limited, so data-based composition-structure-property models are not yet an option. This thesis investigates the composition-structure relation using a statistical mechanical model to capture the enthalpic and entropic contributions to structure formation. This work aims to shed light on the interactions governing structure formation and use this knowledge to model the structure of glasses with unknown compositions.

To investigate the composition-structure relation mentioned above, good-quality structure data is required in multiple glass families. Other than reliable SRO structure characterization, performed by nuclear magnetic resonance (NMR) spectroscopy, chemical composition and glass transition temperature (T_g) should be measured experimentally as these influence the SRO structure. Oxide glass systems investigated in this thesis include a) binary silicate, phosphate, and borate glasses, b) ternary borosilicate, phosphosilicate, and aluminoborate, c) multi-component glasses with Si, P, B, or Al. For a, b, and c, structure, composition, and T_g values were obtained from the literature. Additional $Na_2O-K_2O-SiO_2$ and $Cs_2O-Al_2O3-B_2O_3$ glasses were made for this study by the traditional melt-quenching technique and analyzed by NMR, Inductively coupled plasma (ICP) atomic emission spectroscopy, and differential scanning calorimetry (DSC).

A statistical mechanical model was tailored to predict the SRO structure evolution in the binary oxide glasses by accounting for the enthalpic and entropic contributions to the modifier-former interactions occurring in the glass-forming melt. Good-quality fits were obtained with no more than 1-3 glass compositions as input for the models. The modifier-former interactions captured in binary glasses were then used to predict SRO structures in the ternary glass systems. For example, interactions in Na_2O-SiO_2 and $Na_2O-B_2O_3$ were used to predict structures of $Na_2O-SiO_2-B_2O_3$ glasses. Using binary glass data to predict ternary glass structure worked well for borosilicate and aluminoborate glasses, but in the phosphosilicate glasses, additional interactions occurred between P and Si, which had to be captured. Finally, the statistical mechanical models were combined with machine learning to obtain good structure prediction in unknown glasses. Machine learning learned the composition-structure relation captured by statistical mechanics to reduce the amount of required input data to obtain a good structure prediction.

DANSK RESUME

Der foregår megen forskning og udvikling indenfor oxidglas, men den amorfe struktur af glas betyder at antallet af mulige glassammensætninger er enormt. Databaserede modeller bliver brugt til at accelerere udvilklingen af nye glassammensætninger med specifikke egenskaber ved at etablere en korrelation mellem sammensætning og egenskaber. Disse databasered modeller er ofte begrænsede til sammensætninger tæt på sammensætningerne af data, da relationen mellem sammensætning og egenskaber er kompleks. Atomar glasstruktur har vist sig at korrelere bedre med egenskaber af glas, men mængden af glasstrukturdata er begrænset i forhold til egenskabsdata, så databaserede sammensætning-struktur-egenskabsmodeller er endnu ikke en mulighed. Denne afhandling undersøger sammenhængen imellem glassammensætning og struktur ved hjælp af statistisk mekanik til at fange de entalpiske og entropiske bidrag til formationen af strukturer. Afhandlingen bestræber sig på at kaste lys over de interaktioner, som driver formationen af glasstruktur og bruge denne vide til at forudsige struktur af glas med ukendte sammensætninger.

For at undersøge sammensætning-struktur-forholdet nævnt ovenfor kræves strukturdata af god kvalitet i flere glasfamilier. Andet end pålidelig strukturkarakterisering, udført ved nuclear magnetic resonance (NMR) spektroskopi, bør kemisk sammensætning og glasovergangstemperatur (T_g) måles eksperimentelt, da disse påvirker glasstrukturen. Oxidglassystemer undersøgt i denne afhandling omfatter a) binære silikat-, phosphat- og boratglas, b) ternært borosilikat, fosfosilikat og aluminoborat, c) flerkomponentglas med Si, P, B eller Al. For a, b og c blev struktur, sammensætning og T_g-værdier indsamlet fra litteraturen. Yderligere Na_2O-K_2O-SiO_2- og Cs_2O-Al_2O_3-B_2O_3 glas blev fremstillet til denne undersøgelse ved hjælp af den traditionelle smeltekølende teknik og analyseret ved NMR, induktivt koblet plasma (ICP) atomemissionsspektroskopi og differentiel scanningskalorimetri (DSC).

En statistisk mekanisk model blev skræddersyet til at forudsige strukturudviklingen i de binære oxidglas ved at tage højde for de enthalpiske og entropiske bidrag til modifer-former interaktioner, der forekommer i den glasdannende smelte. Forudsigelse af god kvalitet blev opnået med ikke mere end 1-3 glaskompositioner som input til modellerne. Modifer-former interaktioner ëtableret i binære glas blev derefter brugt til at forudsige strukturer i de ternære glassystemer. For eksempel blev interaktioner i Na_2O-SiO_2 og Na_2O-B_2O_3 brugt til at forudsige strukturer af Na_2O-SiO_2-B_2O_3-glas. Brugen af binære glasdata til at forudsige ternær glasstruktur fungerede godt for borosilicat- og aluminoboratglas, men i fosfosilikatglas optrådte der yderligere interaktioner mellem P og Si, som skulle forstås. De statistiske mekaniske modeller blev kombineret med maskinlæring for at opnå god strukturforudsigelse i ukendte glassammensætninger. Maskinlæring lærte komposition-struktur-forholdet etableret af statistisk mekanik for at reducere mængden af nødvendige inputdata for at opnå en god strukturforudsigelse.

PREFACE AND ACKNOWLEDGEMENTS

This thesis is part two of an integrated Ph.D. project ("4+4 Ph.D. in Danish"). The integrated Ph.D. project is a combined Master's and Ph.D. program, where two separate theses are prepared. Part one, and the Master's thesis, of the project, was handed in and defended after the first two years. While this Ph.D. thesis is one coherent story, some content of the Master's thesis is excluded from the content of this dissertation to avoid plagiarism. Specifically, the three first papers published as a part of this project were included in the Master's thesis, and because of that, they are not part of the official content of this Ph.D. dissertation. However, these papers are still reviewed and referenced to present the entire project.

TABLE OF CONTENTS

CHAPTER 1. INTRODUCTION

1.1. MOTIVATION

Glasses have played a massive role in the rapid the industrial and technological development throughout the ages.[1] Glass was first discovered in the form of obsidian, formed when lava touched water and colored dark due iron and other transition metals. Later, when people started melting metals at high temperatures, glass could form by accident with when sand and coke were kept close to the heat. Like obsidian, this form of glass was of poor quality for any practical application but often possessed colors because of metals and was prized for its transparency. Because of the transparency and coloring, glass beads were used for personal decorations, and later, glass mosaics were used to decorate churches and other important buildings.[2] With transparency and high durability, glass was commonly used for windows in the early 17th century, allowing natural light to enter buildings while protecting the inside against weather and wind.[3] In the 20th century, glass became a high-tech material used in technologies like optical fibers[4,5], nuclear waste encasement[6,7], and bone- and tissue regeneration[8,9].

With the extensive range of high-and low-tech applications of glasses came an increased interest in researching both glass chemistry and post-treatment to tune their physical properties to each use.[10] Here, another challenge arose due to the fascinating state of glasses. Commonly, a liquid becomes solid by crystallizing when the temperature becomes too low for the atoms/molecules in the liquid to rearrange freely.[11] In crystalline materials, the atoms/molecules are connected in crystalline lattices, limiting the components of those materials because of the requirements of the lattice structure. For example, water readily crystallizes into ice because of the 2:1 ratio between hydrogen and oxygen, with hydrogen coordinating to two oxygen and oxygen coordinating to four hydrogens.[11] However, glasses are materials that do not readily crystallize from their parent melts, or are cooled below the melting temperature dater than the crystallization happens, and as such, the components do not follow any fixed ratios.[12] It has previously been estimated that somewhere in the range of 10^{52} different glass compositions are obtainable because many of the elements in the periodic table can form glasses, and the number of different elements can reach beyond twenty.[13]

While traditional trial-and-error methods of finding new glass compositions have been successful, the number of possible glass compositions far exceeds what is feasible to investigate with this method.[14] In recent years, glass development has become increasingly modeling-dependent.[15-17] Here, large datasets with glass compositions and their resulting properties are empirically used to predict new compositions with optimal properties.[18-20] However, the composition to property relation is often complex, so these models are typically limited to interpolating within

the compositions already known.[14] However, short-range order (SRO) structure has recently been found to correlate well with many properties, and structure-property models have been successful in the extrapolative prediction of glass properties.[17,21-23] Unfortunately, obtaining structure data is difficult and time-consuming due to the amorphous nature of glass structure.[24,25] Obtaining a good understanding of the composition-structure relation for glasses would thus allow for better structure-property modeling and enable accurate composition-structure-property modeling. This would be significant for developing new property models as structure knowledge can improve the property prediction of future models.

1.2. SCOPE AND OBJECTIVES

The overall goal of the work presented in this thesis has been to improve the understanding of composition-structure relation in oxide glasses, focusing on SRO structure. Specifically, statistical mechanics was used to capture the energies associated with the formation of structural units in oxide glasses. With the energies governing structure formation established, general composition-structure models were developed. Furthermore, this thesis focused only on oxide glass families as similarities in these systems are similar in their SRO structure, making it the obvious limitation of this work. This thesis aims to elucidate on the following aspects:

- The composition-SRO structure relation in binary oxide glasses
- Statistical mechanics as a tool for structure prediction
- The impact of thermal history on SRO glass structure
- The correlation between binary glass structures and ternary glass structures
- The potential to predict glass structures with state-of-the-art modeling techniques

In this thesis, the essential findings by the author are highlighted with appropriate introductions. First, the thesis introduces the glass formation and atomic-scale structures of common oxide glass families in Chapter 2. In Chapter 3, the statistical mechanics-based model investigated is introduced with practical examples from some of the studies included in the thesis. Chapters 2 and 3 will lay the theoretical foundation for the results discussed in Chapters 4 and 5. In Chapter 4, statistical mechanical modeling is used to find the interaction enthalpies governing the formation of structural units in binary oxide glasses. Additionally, the effect of the thermal history on the glass structure is discussed. In Chapter 5, the enthalpy values obtained in Chapter 4 are used to predict the structures of multi-component glasses with complex structures. In Chapter 6, the main findings are summarized and discussed.

1.3. THESIS CONTENT

The first part of this thesis is an extended summary of the results and discussions reported in scientific papers published in peer-reviewed journals during the project. This thesis is part two of an integrated Ph.D. project. A Master's thesis was prepared and defended after the first two years of the project. Three papers were published during the first part and were included in the Master's thesis. These papers are not included as content in this thesis but will be referred to as "Paper A"[26], "Paper B"[27], and "Paper C"[28]. The papers listed below are part of the thesis content and will be referred to by their roman numerals throughout the thesis.

I.   **Mikkel S. Bødker**, Rasmus Christensen, Luna G. Sørensen, Martin B. Østergaard, Randall E. Youngman, John C. Mauro, Morten M. Smedskjaer, "Predicting Cation Interactions in Alkali Aluminoborate Glasses using Statistical Mechanics", *Journal of Non-Crystalline Solids*, **544** (2020) 120099

II. **Mikkel S. Bødker**, Randall E. Youngman, John C. Mauro, Morten M. Smedskjaer, "Mixed Alkali Effect in Silicate Glass Structure: Viewpoint of ^{29}Si Nuclear Magnetic Resonance and Statistical Mechanics", *The Journal of Physical Chemistry B*, **124** (2020) 10292-10299

III. **Mikkel S. Bødker**, Collin J. Wilkinson, John C. Mauro, Morten M. Smedskjaer, "StatMechGlass: Python based Software for Composition-Structure Prediction in Oxide Glasses using Statistical Mechanics", *SoftwareX*, (In revision)

IV. **Mikkel L. Bødker**, Johan B. Pedersen, Francisco Muñoz, John C. Mauro, Morten M. Smedskjaer, "Statistical Mechanical Model for the Formation of Octahedral Silicon in Phosphosilicate Glasses", *Journal of the American Ceramic Society*, (In revision)

V.   **Mikkel L. Bødker**, Mathieu Bauchy, John C. Mauro, Morten M. Smedskjaer, "Predicting the Structure of Oxide Glasses by Statistical Mechanics-Informed Machine Learning", (Under Preparation)

CHAPTER 2. ATOMIC-SCALE STRUCTURE OF OXIDE GLASSES

2.1. GLASS FORMATION

Most liquids will undergo an abrupt phase transition once reaching a critical temperature during cooling, where the system's internal energy is too low for the atoms to rearrange freely.[29] Crystallization occurs at this temperature (T_m in Figure 2-1), resulting in an abrupt decrease in enthalpy.[11] Some liquids, however, will bypass this critical temperature without crystallizing and become supercooled liquids. Continuous cooling will increase the viscosity of the supercooled liquids until reaching such a high viscosity that the atoms can no longer freely rearrange (T_f in Figure 2-1), and a rigid glass is formed.[30] As shown in Figure 2-1, the fictive temperature is dependent on the cooling rate as the time it takes for the atoms to rearrange is constant at a given temperature, cooling faster than the rearrangement time will result in a glassy structure frozen in at a higher temperature.[31] As such, glasses are solid materials with atomic structures resembling the supercooled liquid at the fictive temperature. The cooling rate will influence the atomic structure of the glass as a glass made with a faster cooling rate will have an atomic structure resembling the supercooled liquid at a higher temperature than a slow-cooled glass. The glass transition temperature (T_g) is generally accepted as the temperature where the glass-forming liquid becomes solid. T_g is defined as the temperature at which the glass-forming liquid reaches a viscosity of 10^{12} Pa×S and is not cooling rate dependent.[30] T_f is estimated to be equal to T_g at a cooling rate of 10K/min.[32]
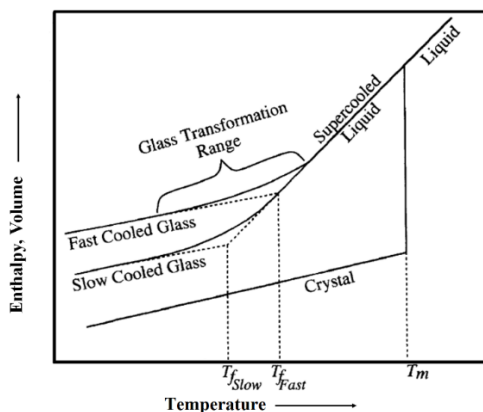

Figure 2-1. Enthalpy of a glass-forming liquid is illustrated as a function of temperature. T_m is the melting temperature of the corresponding crystal, T_{ffast} and T_{fslow} are fictive temperatures obtained with a fast and slow cooling rate, respectively. Figure adapted from literature[29].

Oxide glasses are a subgroup of glasses made from metal oxides by melting at relatively high temperatures and cooling to room temperature.[10] The backbone of oxide glasses is made up of network formers that form covalent bonds to oxygen. Ordinary glass-forming metal oxides include silica (SiO_2), phosphate (P_2O_5), and borate (B_2O_3). The metal cations in these glass systems are linked together through bridging oxygen (BOs), forming three-dimensional networks. Because of the covalent bonds between oxygen and network forming cations, these materials possess high T_m and T_g values and are expensive to produce. To reduce the oxide glasses' working temperatures, where the melt's viscosity is low enough for processing, network modifiers such as Li_2O, Na_2O, and K_2O are added to the glass-forming mixture.[29] These metal oxides form ionic bonds to oxygen and form non-bridging oxygen (NBOs) in the glass forming network. This reduces the connectivity and the number of covalent BOs in the glass and consequently reduces the working temperatures. Other network modifiers such as CaO, ZnO, and CuO are introduced to commercial glasses to alter physical properties or as colorants.[33]

The following sections will address the specific atomic-scale structures found in some typical glass families, which will be considered in this thesis.

2.2. SILICATE NETWORKS

Silica is the most common glass family and is mainly used for bulk glass in windows, containers etc.[34,35] Si atoms are the network forming cations in Silica (SiO_2), forming tetrahedral structural units with 4 BOs in the pure form.[36,37] As glasses possess no ordered structures in the long-range (periodicity over thousands of atoms) and only to some degree in the intermediate-range (periodicity over tens of atoms), the structure of interest in this thesis is in the short-range order (SRO), which refers to only the nearest neighbor of each atom. Intermediate-range order has also been shown to affect glass properties but is harder to characterize and model, thus SRO is the focus of this thesis.[38,39] In the silicate network, the SRO structures refer to the environment of the four oxygen bonded to the central Si atom. The possible structural units are named according to the Q^n naming convention, where n is the number of BOs per Si atom.[40] In pure SiO_2, all Si atoms are bridging through 4 BOs, and the network then consists of only Q^4 structural units. Upon the addition of network modifiers such as Na_2O, NBOs are formed. A Q^3 unit is a Si atom with 3 BOs and 1 NBO, charge stabilized by the Na^+ ion from Na_2O. All possible SRO structural units in the Na_2O-SiO_2 network are shown in Figure 2-2.
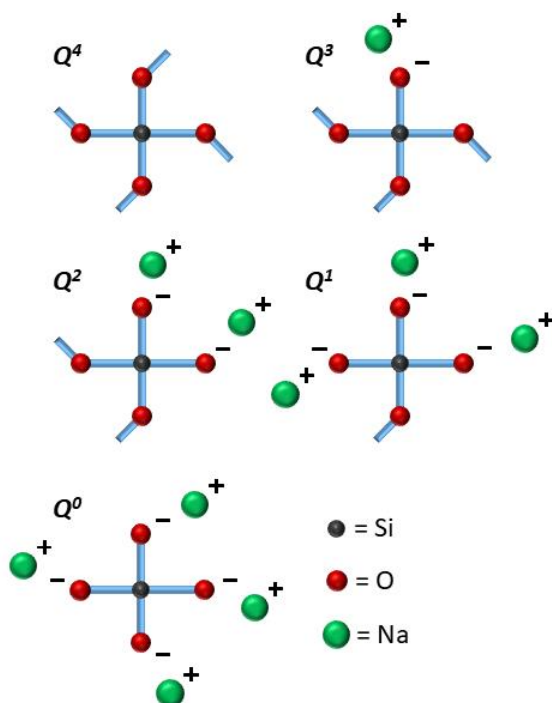
Figure 2-2. Q^n structural units in a Na_2O-SiO_2 glass system. Green symbols are Na^+ ions, red symbols are oxygen atoms, and black symbols are silicon atoms. Covalent bonds are represented by a straight blue line and ionic bonds by the separate charges.

2.3. BORATE NETWORKS

Borate is another common glass family, often used to improve the thermal expansion of the final material.[41] While borate is often used with silica or alumina, binary borate glasses hardly see any commercial use.[42] Boron is found in the 13th periodic table group and has three valence electrons, forming three covalent bonds to obtain a favorable electronic state. The SRO structures are named by the B^n convention (Figure 2-3) for the borate network, where n is the number of BOs on the central B atom.[43] B_2O_3 then consists of only trigonal B^3 units. Upon addition of modifier ions to the B^n network, BOs may be broken to form NBOs and B^{n-1} units similarly to the silicate network. However, a B^3 unit can also be converted to a tetrahedral B^4 unit with 4 BOs and charge-stabilized by the network modifier. This is known as the boron anomaly as the
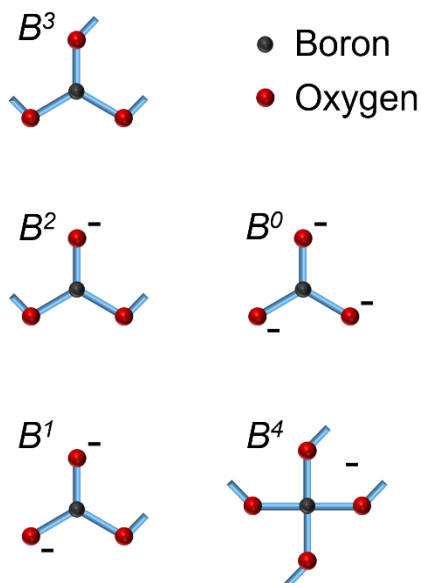
Figure 2-3. B^n structural units in M_2O-B_2O_3 glass. Red symbols are oxygen atoms, and black symbols are boron atoms. A straight blue line represents covalent bonds, and M+ modifier ions balance negative charges.

2.4. PHOSPHATE NETWORKS

Phosphorous is found in the 15th group of the periodic table and has five valence electrons to form five covalent bonds to obtain a favorable electronic state. Since the tetrahedral configuration is favorable, P_2O_5 forms Q^3 units with three BOs and terminal oxygen with a double bond to the central P atom, as seen in Figure 4.[44] The phosphate units are found in tetrahedral configurations. Like the silicate units, they are named using the Q^n convention, where n refers to the number of BOs associated with the central P atom.[45] In future Sections where both Si Q^n and P Q^n units are referenced, these will be referred to as Si^n and P^n, respectively. The addition of modifier ions to the P_2O_5 system breaks BOs to form NBOs, and Q^n units become Q^{n-1} units.
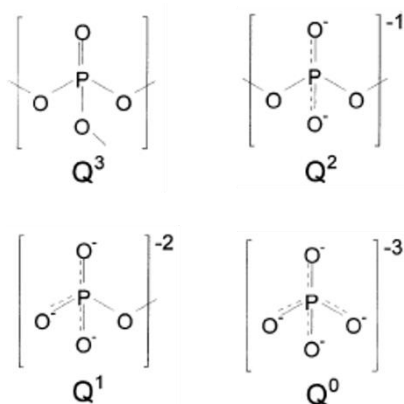
Figure 2-4. Phosphate Q^n structural units in M_2O-P_2O_5 glass, where M refers to an alkali metal. Negative charges on oxygen are partial charges, while the outer charge is the total charge of the unit. Total negative charges are charge-stabilized by M^+ ions.

2.5. BOROSILICATE NETWORKS

Borosilicate glasses consist of both borate and silicate as network formers and any number of network modifiers, making it the first mixed network former glass family reviewed in this thesis. Borosilicate is one of the most commonly used mixed former glass families with uses in high-temperature glassware. The possible SRO structures of borosilicate glasses are summarized in Figures 2-2 and 2-3. As such, the number of possible SRO structures significantly increases when multiple network formers are included in a glass. As these structure units are formed by network modifiers interacting with the different sites, the number of interactions also increases, and consequently, calculating each interaction probability becomes more challenging, as explained later in Section 5-1.

2.6. ALUMINOBORATE NETWORKS

Aluminoborate glasses are interesting from a structure point for both the borate units exhibiting the boron anomaly described in Section 2.3 and the aluminum units. As described in Section 2.2, cations in oxide glasses form either covalent or ionic bonds to oxygen depending on the difference in electronegativity between oxygen and the cation. There is no exact division, so some cations termed network intermediates may form covalent or ionic bonds depending on the chemical environment in the glass-forming melt. Aluminum is an example of a network intermediate and may form either 4-fold coordinated Al^4 units with 4 BOs or 5/6-fold coordinated Al^5/Al^6 units with three ionic bonds and an ionic charge of +3 illustrated in Figure 2-5.
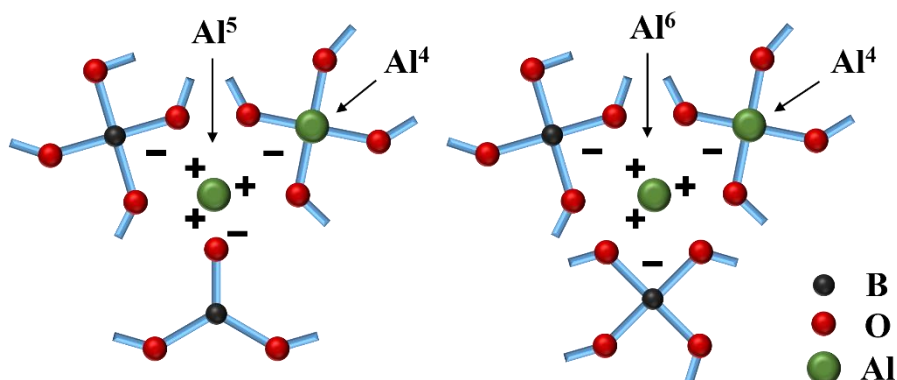
Figure 2-5. Alumina Al^n structural units in M_2O-Al_2O_3-B_2O_3 glass, where M refers to an alkali metal. Negative charges on oxygen are partial charges, while the outer charge is the total charge of the unit. Total negative charges are charge-stabilized by M^+ ions. Figure adapted from Paper I.

2.7. PHOSPHOSILICATE NETWORKS

Phosphosilicate is another exciting glass system studied in paper IV. The structures of the network formers mixed in phosphosilicate glasses, silica and phosphate, are presented for their binary glass systems in Figures 2-2 and 2-4. In addition to the typical structure units found in the binary systems, 6-fold coordinated silicon (Si^6) can also be found in phosphosilicate glasses.[46,47] Figure 2-6 illustrates a reaction between silicon and phosphorous structure units to form the Si^6 unit proposed in literature.[48] Si^6 influences the physical properties of the glasses, such as hardness, and understanding the formation of Si^6 can help design new glass compositions in the future.[49,50]
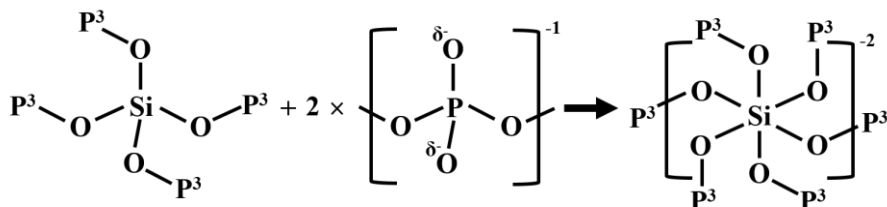
Figure 2-6. The reaction between silicon and phosphorous for the formation of sixfold-coordinated silicon units in phosphosilicate glasses. Figure adapted from Paper IV.

CHAPTER 3. STATISTICAL MECHANICAL MODEL OF SRO STRUCTURE

In this section, we will explore how statistical mechanics can be used to calculate the interaction probabilities for modifier-former interactions and consequently calculate the structure distribution in the glasses. The fraction of SRO structural species in oxide glasses will be calculated as a function of composition and thermal history. The model proposed by Mauro[51] will be reviewed, and some practical applications will be used as examples for the modeling procedure.

As described in Chapter 2, the reaction between network modifiers and formers results in new structural units. These units are of lower potential energy than before the reaction. The lower potential energy after the reaction is a sum of the change of enthalpy and entropy.[52] A modifier ion can undertake multiple reactions in a glass consisting of multiple structural units, resulting in different structural outcomes. Here, one reaction will be enthalpically favorable over the other. However, entropically, it would be favorable for the reactions to occur entirely randomly, forming a broad distribution of structural units.

Consequently, enthalpy and entropy compete to control the former-modifier interactions. As entropy scales with temperature, glass-forming liquids will consist of more randomly distributed structures at high temperatures than at low temperatures. When considering the structure distribution in oxide glasses at room temperature, the structure is assumed to be frozen at T_f. Enthalpy, entropy, and T_f must be accounted for when calculating the interaction probabilities resulting in the final structures at room temperature.

3.1. CALCULATING INTERACTION PROBABILITIES

The key feature of the above-mentioned statistical mechanics approach is that the distribution of structural units in simple oxide glasses can be described using a hypergeometric distribution. Hypergeometric distributions are used to describe the probabilities of a series of events, considering the previous event.[53] If the interaction between a modifier and a network-former species could be assumed to be entirely entropically controlled (e.g., no difference in the preference for a Na^+ modifier ion to interact with Si or B network formers), the regular hypergeometric distribution would capture the distribution of structural units as a function of glass composition. However, in a real system, the modifier-former interactions are also affected by enthalpic contributions, with the system approaching the lowest possible

potential energy, and the regular hypergeometric distribution is thus insufficient. The enthalpic driving force for a modifier-former interaction is captured by using a type of non-central hypergeometric distribution, where each possible event is corrected by a weighting factor specific to that event. Such distribution is described mathematically by the Wallenius type non-central hypergeometric distribution:

$$p_{i,\omega} = \frac{(g_i - n_{i,\omega-1})w_i}{\sum_{j=1}^{M}\sum_{\omega=0}^{\omega-1}(g_j - n_{j,\omega-1})w_i},$$

(3-1)

where $p_{i,\omega}$ is the probability of drawing species i after ω draws, g_i is the initial population of specie i, $n_{i,\omega-1}$ is the number of species i already drawn before draw ω, and w_i is the weighting factor for specie i. The numerator in Eq. 3-1 is the number of species i before the given draw multiplied by the weighting factor of species i, and the denominator in Eq. 3-1 is the total number of species before the draw multiplied by each of their respective weighting factors.

We recall that the non-central hypergeometric distribution is derived from the Boltzmann distribution function to allocate a physical meaning to the weighting factors.[54] In statistical mechanics, this central function describes the probability for a system to be found in a given state as a function of the system's temperature and the energy of that state,

$$p_i = \frac{exp\left(-\frac{\varepsilon_i}{kT}\right)}{\sum_{j=1}^{M}exp\left(-\frac{\varepsilon_j}{kT}\right)},$$

(3-2)

where p_i is the probability of state i, k is the Boltzmann constant, T is the system's temperature, ε_i is the total energy of state i, and M is the total number of states. Recently, Mauro proposed to use the Boltzmann distribution to describe the modifier-former interactions in mixed former oxide glasses.[51,55] With Mauro's model, the probability states (p_i) are defined as interactions between modifier ions and network former species i. Consequently, ε_i becomes the free energy of this interaction. The latter may be described by entropic (S) and enthalpic (H) contributions,

$$p_i = \frac{exp\left(-\frac{H_i - S_i T}{kT}\right)}{\sum_{j=1}^{M}exp\left(-\frac{H_j - S_j T}{kT}\right)}.$$

(3-3)

Next, we define the statistical entropy of the system as,

$$S_i = k\ ln\ \Omega_i\ ,$$

(3-4)

where Ω_i refers to the number of microstates consistent with a given macrostate for species i,

$$p_i = \frac{exp\left(-\frac{H_i - kln\Omega_i T}{kT}\right)}{\sum_{j=1}^{M} exp\left(-\frac{H_j - kln\Omega_j T}{kT}\right)}. \tag{3-5}$$

We then obtain,

$$p_i = \frac{exp\left(-\frac{H_i}{kT} + ln\Omega_i\right)}{\sum_{j=1}^{M} exp\left(-\frac{H_j}{kT} + ln\Omega_j\right)}, \tag{3-6}$$

which can be rewritten as,

$$p_i = \frac{\Omega_i exp\left(-\frac{H_i}{kT}\right)}{\sum_{j=1}^{M} \Omega_j exp\left(-\frac{H_j}{kT}\right)}. \tag{3-7}$$

The number of microstates consistent with the macrostate of units i divided by the total number of microstates consistent with the macrostate of the glass system is the same as the relative fraction of structure unit i divided by the total number of units. Since the amount of a given structural species i in the glass system alters with composition, we get

$$\Omega_{i,\omega} = (g_i - n_{i,\omega}), \tag{3-8}$$

where ω represents a given modifier fraction, g_i is the degeneracy of units i and $n_{i,\omega}$ is the total amount of species i that has already reacted at glass composition ω. When calculating the interaction probability of a unit i at concentration ω, we must use the amount of species i at the previous glass composition (ω-1),

$$p_{i,\omega} = \frac{(g_i - n_{i,\omega-1})exp\left(-\frac{H_i}{kT}\right)}{\sum_{j=1}^{M}\sum_{\omega=0}^{\omega-1}(g_j - n_{j,\omega-1})exp\left(-\frac{H_j}{kT}\right)}. \tag{3-9}$$

The double summation in the denominator is over all species M and each modifier concentration ω up to, but not including, the current concentration ω. The probability distribution function shown in Eq. 3-9 is a type of non-central hypergeometric distribution function, where enthalpy values (H_i) are the free parameters obtained by fitting to experimental data. Next, we define $exp\left(-\frac{H_i}{kT}\right)$ as the weighting factor w_i for the probability of a modifier to react with structural unit i, where T is assumed to be T_f for $T < T_f$, since the structure is assumed to freeze in at the fictive temperature:

$$p_{i,\omega} = \frac{(g_i - n_{i,\omega-1})w_i}{\sum_{j=1}^{M}\sum_{\omega=0}^{\omega-1}(g_j - n_{j,\omega-1})w_j}, \tag{3-10}$$

where,
$$w_i = exp\left(-\frac{H_i}{kT_f}\right).$$
<div align="right">*(3-11)*</div>

In this thesis, this approach has been utilized to calculate the average concentration of structural units as a function of the glass composition. It was discovered that the model of Eqs. 3-10 and 3-11 can be fitted to experimentally obtained mechanical data of simple, binary oxide glass systems to obtain H_i values specific to each modifier-structural unit pair. Besides the average structure, recent studies have found that the approach is also well suited to calculate and exploring structural fluctuations in glass-forming liquids by computing the probability distribution function of modifier-former interactions. By iterating over Eq. 3-10, a standard deviation to the mean probability can be obtained to measure the degree of structural fluctuations.[56-58]

3.2. INTERACTION PROBABILITIES TO ABSOLUTE FRACTIONS

In this section, the connection between the interaction probabilities calculated in Section 3.1 and the final structure of the glass is described. The fraction of structural units i at ω is calculated from the fraction of those species at ω-1 and $p_{i,\omega}$ values that depend on fraction at ω-1. Then, the latest structural fraction at ω is used to calculated probabilities $p_{i,\omega+1}$. It is possible to iteratively calculate the fraction of all structural units at all modifier concentrations ω by knowing a starting fraction of structural units at ω=0 if w_i for all i are known. Otherwise, the model is fitted to experimentally obtained data to obtain w_i. The Q^n distribution in Na_2O-SiO_2 is shown in Figure 3-1 after the first draw, where the colored spheres illustrate each Q^n unit. After the first draw, the probability of drawing another Q^4 unit remains 1 when rounded to 3 decimals. This is caused by the weighting factors in the bottom right corner of the Figure.

Figure 3-1. The probabilities of drawing a network-former unit at 0 % modifier in a Na_2O-SiO_2 glass system. The colored spheres illustrate the fraction of structural units in the glass at the first draw. The top right graph has experimental data of composition-structure relation as symbols and model prediction as lines (up until the current concentration). The lower right graph illustrates T_g at the composition as a line and the weighting factors for the given composition calculated with the T_g value. As the concentration of Na_2O in this example is 1 mol%, the lines in the graphs are just starting to form.

In Figure 3-2, the drawing probabilities for each structural unit are calculated for a $50Na_2O$-$50SiO_2$ glass. Note how the probability of drawing a Q^3 unit is higher than drawing a Q^2 unit despite the more significant fraction of Q^2 units. Figures 3-1 and 3-2 should illustrate the numerical solution to calculating the interaction probabilities. Knowing the starting fraction and the starting weighting factors allows for calculating the initial probabilities. From the initial probabilities, the concentration of each unit randomly picked for interaction is known, and the new fractions may be calculated, as these units are returned to the population as different units. In the bottom right corner of Figure 3-2, the T_g of the glass composition is shown and used to calculate new weighting factors iteratively. Note the change in the weighting factors between Figures 3-1 and 3-2 due to the difference in T_g.
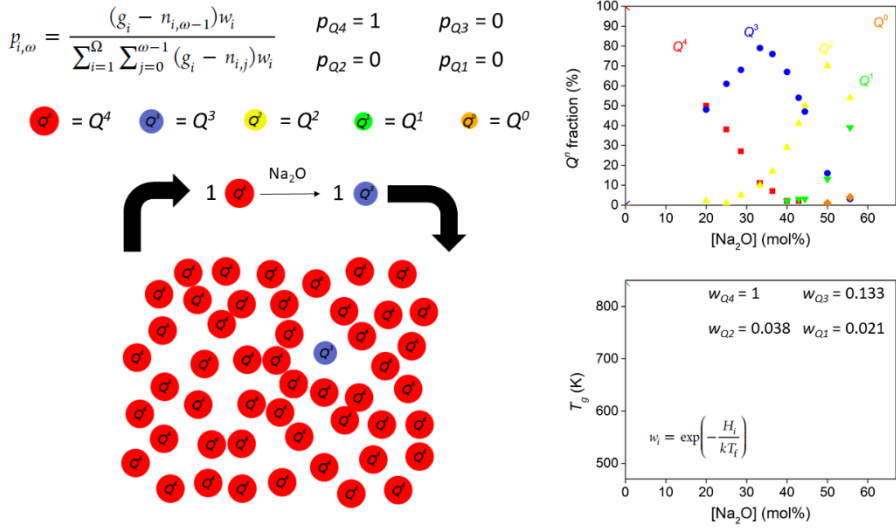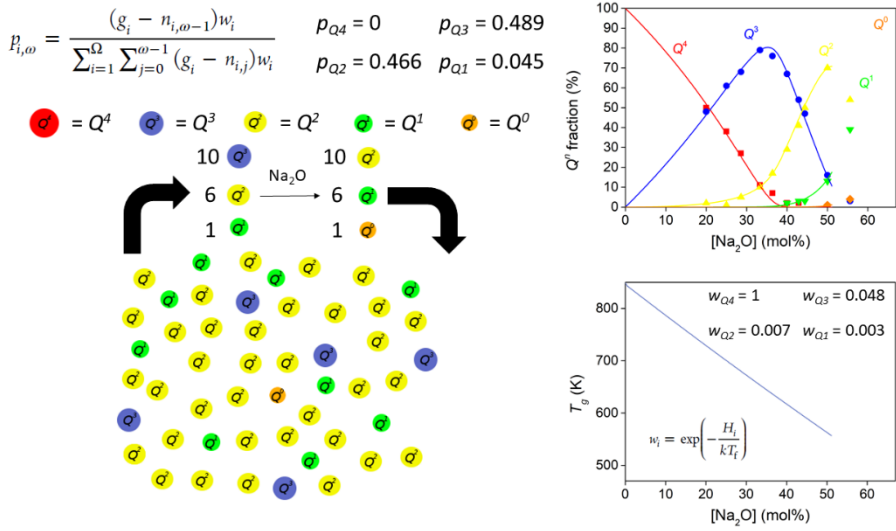
Figure 3-2. The probabilities of drawing a network-former unit at 50 % modifier in a Na₂O-SiO₂ glass system. The colored spheres illustrate the fraction of structural units in the glass at the first draw. The top right graph has experimental data of composition-structure relation as symbols and model prediction as lines (up until the current concentration). The lower right graph illustrates T_g at the composition as a line and the weighting factors for the given composition calculated with the T_g value.

If the T_g values of the glass are known, the model can be used to obtain the H_i of modifier former interactions. Assuming that the H_i values are constant for the modifier-former interaction, they can be used in all glasses where that interaction occurs. The model can then be fitted to structure data of simple glass systems to obtain H_i values from, which can be used to predict structural evolutions in multi-component glasses without additional fitting.

CHAPTER 4. COMPOSITION-STRUCTURE MODELING IN BINARY OXIDE GLASSES

4.1. EXTRACTING REACTION ENTHALPIES FROM STRUCTURE DATA

Figure 4-1 illustrates each unit's compositional structure evolution in binary alkali phosphates (Paper A) as predicted by the chemical order model.[59] As seen in Figure 4-1, this model assumption expects a stepwise conversion of the Q^n units in phosphates with increasing modifier concentration. This assumption is backed by the oxygen double bond delocalizing to any NBO. The Q^2 structure is more energetically favorable than the Q^3 structure. The energy difference between a Q^3 and Q^2 is more significant than between Q^2 and Q^1, making the Q^2 less likely to react with a modifier. By fitting the statistical mechanics-based model shown in Section 3.1 to experimentally obtained structure data, the enthalpies of these interactions are obtained, allowing for composition-structure prediction specific to each glass system. Obtaining good-quality structure data can be challenging, and nuclear magnetic resonance spectroscopy is the only widely acknowledged method of quantifying SRO structures in oxide glasses.[60] The chemical composition can also change slightly during glass melting because of vaporization, so measuring the chemical composition is crucial for good-quality structure data. Finally, T_g or T_f must be known, or the glass must be annealed at a known temperature to predict the structures with statistical mechanics.
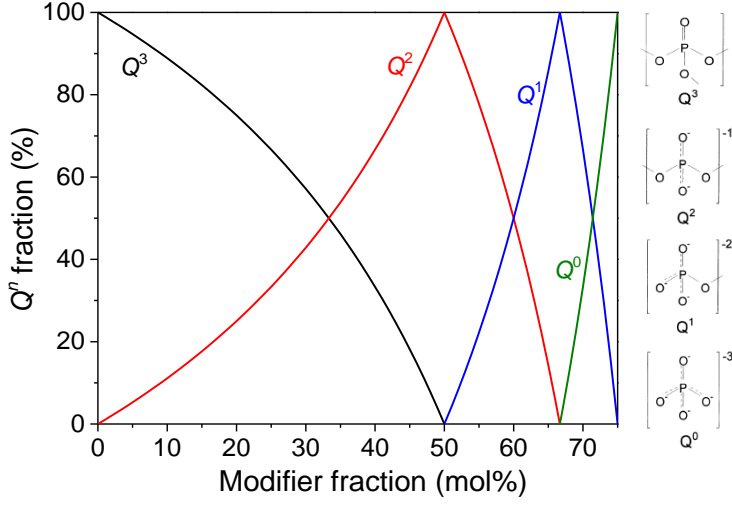
Figure 4-1. The fraction of Q^n structural units as a function of composition for alkali phosphate glasses as predicted by the chemical order model. Reprinted with permission from Paper A[26]. Copyright 2021 American Chemical Society

To implement the phosphate structures in the statistical mechanical model, let us define the probability for a sodium modifier to interact with a Q^3 unit at a glass composition ω, with the interaction enthalpies as free parameters:

$$p_{Q^3,\omega} = \frac{Q^3_{\omega-1} w_{Q^3,\omega}}{Q^3_{\omega-1} w_{Q^3,\omega} + Q^2_{\omega-1} w_{Q^2,\omega} + Q^1_{\omega-1} w_{Q^1,\omega}}, \qquad (4\text{-}1)$$

where,

$$w_{Q^3,\omega} = e^{-\frac{H_{Na^+,Q^3}}{kT_{f_\omega}}}, \qquad (4\text{-}2)$$

where H_{Na^+,Q^3} is the enthalpy value for sodium to react with a Q^3 structural unit, T_{f_ω} is the fictive temperature at glass composition ω, and k refers to the Boltzmann constant (in kJ mol^{-1} K^{-1}). The same method calculates the probabilities modifier interactions for Q^2 and Q^1 at glass composition ω.

Then, the fractions of Q^3, Q^2, Q^1, and Q^0 at composition ω are calculated:

$$Q^3_\omega = Q^3_{\omega-1} - p_{Q^3,\omega}, \qquad (4\text{-}3)$$

$$Q^2_\omega = Q^2_{\omega-1} + p_{Q^3,\omega} - p_{Q^2,\omega}, \qquad (4\text{-}4)$$

$$Q_\omega^1 = Q_{\omega-1}^1 + p_{Q^2,\omega} - p_{Q^1,\omega}, \qquad (4\text{-}5)$$

$$Q_\omega^0 = Q_{\omega-1}^0 + p_{Q^1,\omega}. \qquad (4\text{-}6)$$

Here, the concentration of Q^3, Q^2, and Q^1 units will decrease for each draw ω relative to the probabilities for drawing those species, and the fractions of Q^2, Q^1, and Q^0 will increase with the probability of drawing Q^3, Q^2, and Q^1 units, respectively. Since Q^3 transitions to Q^2, a modifier's probability of interacting the Q_ω^n fractions are then used to calculate probabilities at glass concentration $\omega+1$ etc.

Figure 4-2 shows prediction by the statistical mechanics-based model (Paper A) and ^{31}P NMR data from Li_2O-P_2O_5 glasses.[61,62] The model was fitted on structural data of only one glass ($50Li_2O$-$50P_2O_5$) yet fitted very well with all the data. The enthalpies of all the interactions obtained by fitting the model are reported in Table 4-1.

Figure 4-2. The concentration of Q^n structural units in lithium phosphate glasses as a function of composition. Experimental data from literature is represented as closed and open symbols, respectively. Solid lines represent prediction using the statistical mechanics-based model, established only based on data of the glass indicated by an arrow. Reprinted with permission from Paper A[26]. Copyright 2021 American Chemical Society

Glass modifier	Li_2O	Na_2O	Cs_2O	MgO	ZnO
H_3 (kJ/mol)	0	0	0	0	0
H_2-H_3 (kJ/mol)	33.5	42.8	56.8	31.6	27.0
H_1-H_3 (kJ/mol)	70.4	74.9	85.1	55.0	40.0
R^2	0.992	0.998	0.996	0.942	0.988

Table 4-1. H_i parameters and R^2 values were obtained by fitting the present model to experimental data in five phosphate glass systems. H_i values scale according to the Q^3 to Q^2 conversion (H_3), defined as 0. Reprinted with permission from Paper A[26]. Copyright 2021 American Chemical Society

The next part focuses on predicting the structure of silicate glasses (Paper C). Structural Q^n units observed in silicate glasses are shown in Figure 2-2. The SRO units interact with modifier ions similarly to phosphate glasses:

$$Q_\omega^n = Q_{\omega-1}^n + p_{Q^{n+1},\omega} - p_{Q^n,\omega}, \qquad (4\text{-}7)$$

where Q_ω^n is the amount of Q^n at draw ω, and the probabilities $p_{Q^n,\omega}$ are calculated as:

$$p_{Q^n,\omega} = \frac{Q_{\omega-1}^n w_{Q^n,\omega}}{\sum_{n=1}^N Q_{\omega-1}^n w_{Q^n,\omega}}, \qquad (4\text{-}8)$$

where N is the total number of structural units. $w_{Q^n,\omega}$ is defined as:

$$w_{Q^n,\omega} = e^{-\frac{H_{M^+,Q^n}}{kT_{f_\omega}}}. \qquad (4\text{-}9)$$

Like in the phosphate glasses, the enthalpy values for modifier-structure interaction is obtained by fitting the model to structural data.

Figure 4-3 shows the compositional evolution of Q^n units in Na_2O-SiO_2 glasses as obtained by ^{29}Si MAS-NMR experiments.[63] Model predictions show an excellent agreement to structure data.
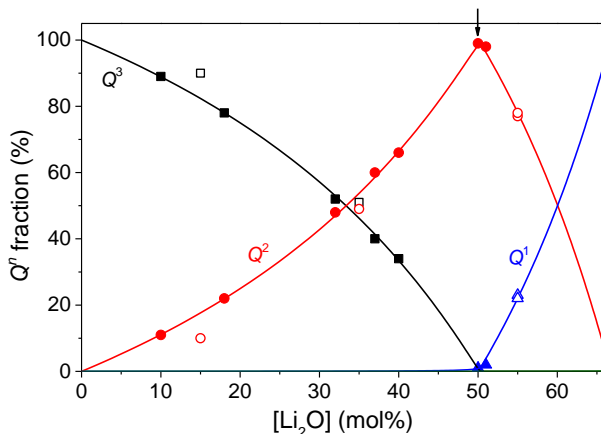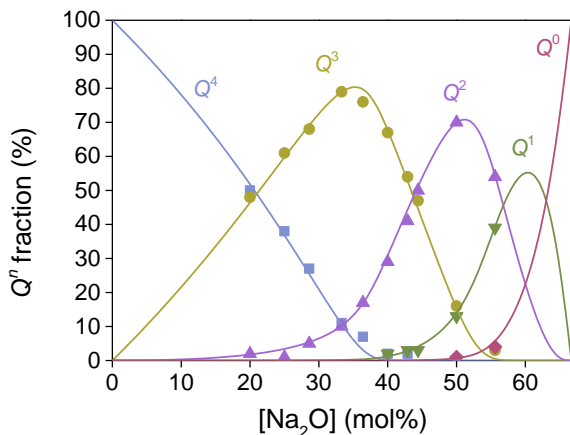
Figure 4-3. The concentration of Q^n structural units in sodium silicate glasses as a function of composition. Experimental data from literature are represented as symbols, and solid lines represent model prediction using the statistical mechanics. Reprinted from Paper C[28] under the Creative Commons Attribution License.

Glass modifier	Li_2O	Na_2O	K_2O
H_4 (kJ/mol)	0	0	0
H_3-H_4 (kJ/mol)	8.4	14.1	18.8
H_2-H_4 (kJ/mol)	16.4	22.9	35.5
H_1-H_4 (kJ/mol)	22.1	27.1	45.8

Table 4-2. H_i parameters were obtained by fitting the present model to experimental data in three different silicate glass systems. H_i values scale according to the Q^4 to Q^3 conversion (H_4), defined as 0. Reprinted from Paper C[28] under the Creative Commons Attribution License.

As was the case for phosphate glass, the higher the field strength of the modifier, the more significant the enthalpy difference between the interactions (Table 4-2). This is explained by a higher degree of disproportionation of structural units in the Li_2O-SiO_2 glasses than Na_2O-SiO_2 or K_2O-SiO_2.[63]

4.2. FICTIVE TEMPERATURE

Molecular dynamics (MD) simulation is another method to investigate the SRO scale structure of glasses.[64,65] A significant drawback of MD is very short simulation timescales (nanoseconds to a few microseconds).[31] Because of the short simulation timescales, glasses made with MD will attain unrealistically high T_f values, and the distributions of SRO structures differ significantly from glasses investigated by NMR

experiments. Since the statistical mechanics-based model uses T_f as an input parameter, it can be a tool to compare MD simulated glass structures with melt-quenched glass structures as will be examined in the next section.

In Figure 4-4, the distribution of predicted SRO structures in a $35Na_2O\text{-}65SiO_2$ glass is plotted against temperature. The distribution of Q^n units in the same glass as obtained by MD simulations fits precisely with the prediction made by statistical mechanics.[64,66] This is a strong indication that the model results of the statistical mechanics-based model may be used to describe both MD simulated- and melt-quenched glasses.
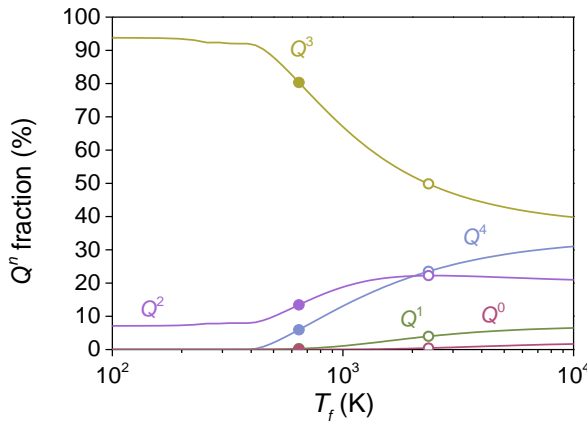
Figure 4-4. SRO structures in 35Na₂O-65SiO₂ were plotted as a function of Tf. Open symbols represent MD simulated data. Closed symbols represent experimental data obtained by ²⁹Si MAS-NMR. Solid lines represent model predictions. Reprinted from Paper C[28] under the Creative Commons Attribution License.

Figure 4-5 shows structure prediction of MD simulated glass data with statistical mechanics, using the enthalpy values obtained in experimentally obtained $Na_2O\text{-}SiO_2$ glass (Paper C). The model fits the structural evolution of MD simulated $Na_2O\text{-}SiO_2$ glasses very well while only scaling the T_f as a free parameter (MD $T_f = 3.6 \times T_g$).
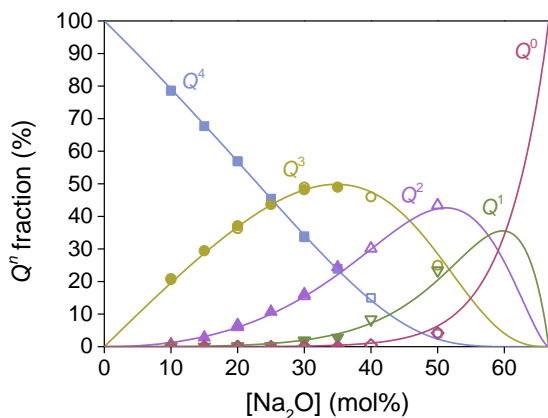
Figure 4-5. The concentration of Q^n structural units plotted against composition in sodium silicate glasses. Closed and open symbols represent data from MD simulations. Solid lines represent model predictions, using the enthalpy parameter shown in Table 4-2 but a different fictive temperature than Figure 10. Reprinted from Paper C[28] under the Creative Commons Attribution License.

The statistical mechanics-based model was fitted successfully to experimentally obtained structure data in the binary silicate glass system. The temperature dependence of the statistical mechanics-based model was used to calculate composition-structure relations for MD simulated glasses without changing enthalpy parameters from those obtained by fitting to MAS-NMR spectroscopy of melt-quenched glasses.

4.3. MIXED MODIFIER EFFECT IN SILICATE GLASSES

The mixed modifier effect refers to the non-linear relation of any glass property with the ratio between two modifiers while keeping the remaining composition constant.[2,67,68] In Paper II, a series of Na_2O-K_2O-SiO_2 glasses were made with varying modifier ratios at three different SiO_2 concentrations. All glasses had their chemical composition measured by inductively coupled plasma spectroscopy and T_g by differential scanning calorimetry. Then, the structures were measured by solid-state nuclear magnetic resonance spectroscopy. With the compositions and T_g values, the statistical mechanical model was used to calculate the structural units of the mixed modifier glasses by using enthalpies obtained in binary Na_2O-SiO_2 and K_2O-SiO_2 glasses, respectively. The model showed excellent agreement with the experimental structure data, and with the parameters and T_g values, the mixed modifier effect on structures was investigated, as shown in Figure 4-6. We found that the mixed alkali effect on structural units contributes to the T_g variation, which exhibits a non-linear variation when one alkali is substituted for another one while keeping the total modifier concentration constant. As the T_g decreases from the linear correlation when

mixing modifiers in the silicate glass system, the entropic effect on the structural distribution decreases, resulting in a less disordered distribution as captured by the statistical mechanical model.
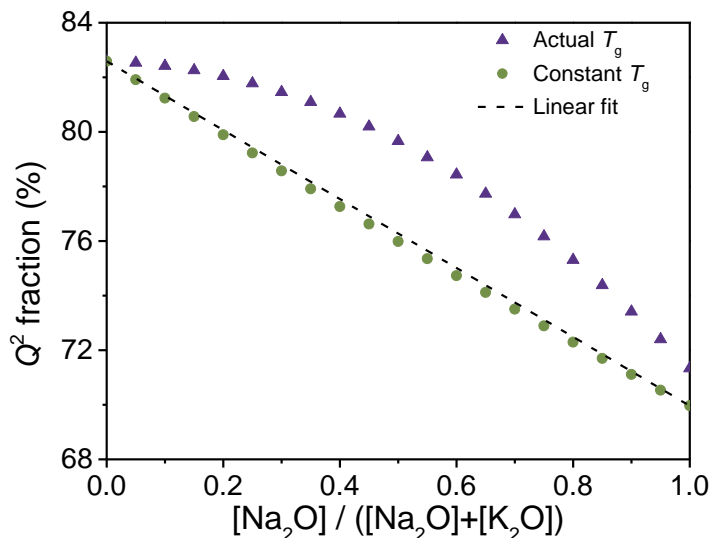
Figure 4-6. Fraction of Q^2 species as a function of the sodium oxide to total modifier oxide content for the 50M2O-50SiO2 glasses. The solid symbols represent fractions of Q^2 species predicted by the statistical mechanics-based model with constant T_g (circles) or the actual measured T_g (triangles). The dashed line represents a linear fit between to the data for Q^2 fractions of 50Na2O-50SiO2 and 50K2O-50SiO2 glasses. Reprinted with permission from Paper II. Copyright 2021 American Chemical Society.

CHAPTER 5. COMPOSITION-STRUCTURE MODELING IN MULTI-COMPONENT OXIDE GLASSES

With the application of the statistical mechanical method described in Chapter 4, the modifier-former interaction enthalpies are established by fitting the model to structural data in binary glasses. This section will explore how the parameters obtained in binary glass systems can be used directly to calculate the structure distribution of multi-component glasses without fitting to the structure of multi-component glasses. For example, the enthalpy parameters obtained in the Na_2O-SiO_2 and Na_2O-P_2O_5 glasses in Section 4 are used to describe the reaction probabilities between sodium and both Si and P structural units. Assuming the same reactions in a Na_2O-SiO_2-P_2O_5 glass system, those parameters can be applied in calculating the structural distributions in the ternary glass system without any fitting. As the following Sections will explore, former-former interactions often occur in the mixed former glass systems, complicating the model slightly. These additional interactions can be captured either by introducing additional parameters for each former-former pair or all at once using a neural network machine learning approach. Both of these options are investigated in this section.

5.1. STRUCTURE PREDICTION IN BOROSILICATE GLASSES

The SRO structures observed in borosilicate glasses are summarized when combining Figures 2-2 and 2-3.[69-71] When modeling the SRO structures in ternary borosilicate glasses (Paper C), the modifier interaction with a structural unit is assumed to be identical to the modifier-former interactions in binary glasses. The difference is in the competitional factor since more different units compete in interaction with the modifier. The denominator of Eq. 3-9 becomes different, but the numerator is the same as for binary glasses. The denominator captures all structure units at once, while the numerator accounts for only one structure unit at once.

The enthalpy values for binary borates (Paper B) and silicates (Paper C) are reported in Table 5-1. Na_2O-SiO_2 and Na_2O-B_2O_3 enthalpies were used to predict the SRO structures in Na_2O-B_2O_3-SiO_2 glasses. All parameters are relative to binary systems, as seen in Table 5-1, where H_4 values are set to 0 and must be corrected for the Si/B preference of the modifier. The Si/B weighting factor is obtained by fitting the model with only this one free parameter.

Glass system	Na$_2$O-SiO$_2$	K$_2$O-SiO$_2$	Na$_2$O-B$_2$O$_3$	K$_2$O-B$_2$O$_3$
H_4 (kJ/mol)	0	0	0	0
H_3-H_4 (kJ/mol)	14.1	18.8	8.4	6.0
H_2-H_4 (kJ/mol)	22.9	35.2	7.4	21.4
H_1-H_4 (kJ/mol)	27.1	32.8	28.5	28.3
α_{B^4/B^2}	-	-	35.5	35.4

Table 5-1. Relative enthalpies (H_i), where i refers to a given structural unit. The following structural units are considered: Q^4, Q^3, Q^2, and Q^1 for i = 1, 2, 3, and 4, in the silicate glasses and B^3, B^4, B^2 and B^1 for i = 1, 2, 3, and 4, in the borate glasses. Reprinted from Paper C[28] under the Creative Commons Attribution License.

To establish the borate enthalpies, the following interactions were considered:

$$2B^3 + M_2O \rightarrow 2B^4, \qquad (5\text{-}1)$$

$$2B^3 + M_2O \rightarrow 2B^2. \qquad (5\text{-}2)$$

Eqs. 5-1 and 5-2 account for the boron anomaly. The α_{B^4/B^2} parameter accounts for a critical modifier concentration. At this concentration, Eq. 5-1 stops occurring in place of Eq. 5-2. In reality, these reactions occur more simultaneously, but this assumption allows for accurate prediction with only one additional parameter.

$$2B^4 + M_2O \rightarrow 2B^2 + M_2O. \qquad (5\text{-}3)$$

B^4 will start to become B^2 units when interacting at high modifier concentrations. Eq. 5-3 is assumed to be a reaction with a corresponding enthalpy parameter to account for this anomaly.

$$2B^2 + M_2O \rightarrow 2B^1, \qquad (5\text{-}4)$$

$$2B^1 + M_2O \rightarrow 2B^0. \qquad (5\text{-}5)$$
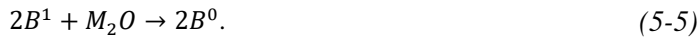
With the interactions established and the parameters obtained from fitting the model to experimental data from literature[63,72-74], borosilicate structures were calculated using the statistical mechanics-based approach and compared to glass structures obtained experimentally.[75-77]

As seen in Figure 5-1, the model does not capture the structural data in Na$_2$O-B$_2$O$_3$-SiO$_2$ glasses obtained by NMR. Deconvoluting NMR results in this system is complex, and the uncertainty of experimental data is high. Another method of obtaining SRO structural data is by MD simulations. As shown in Section 4.2, the enthalpy values obtained by statistical mechanics applies to MD simulated glasses

when accounting for the different T_f value. As such, MD may serve as a more accurate reference with minimal uncertainty.
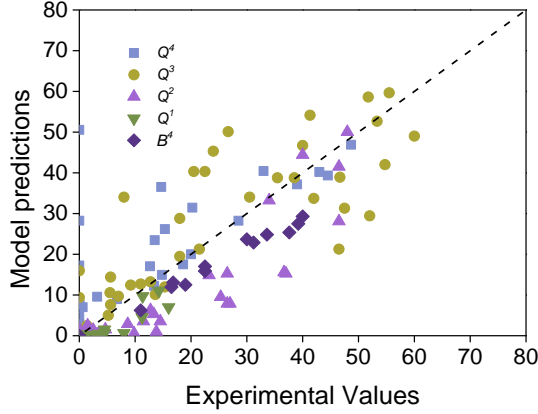
Figure 5-1. Structure data obtained by ^{29}Si and ^{11}B MAS NMR in literature for sodium borosilicate glasses, compared to model predictions. The dashed line represents a one-to-one correlation. Reprinted from Paper C[28] under the Creative Commons Attribution License.

When fitting the model to MD simulated glass structures[78] (Paper C), the statistical mechanics-based model captures the structural evolution very well (Figure 5-2). The Si/B weighting ($w_{Si,B}$=0.16) was the only free parameter.

Figure 5-2. Structure data obtained by MD simulations in literature for sodium borosilicate glasses, compared to model predictions. The dashed line represents a one-to-one correlation. Reprinted from Paper C[28] under the Creative Commons Attribution License.

With $w_{Si,B}$ established, the model may be used to calculate the structures of any borosilicate glass with no free parameters. Next, K_2O-SiO_2- and K_2O-B_2O_3 parameters were established by fitting the model to structural data from literature[79-82] as explained in this section. With the new parameters, the structure of K_2O-B_2O_3-SiO_2 glasses was predicted without any fitting. To investigate the predictions without any fitting, MD simulations of K_2O-B_2O_3-SiO_2 glasses were made (Paper C) by already established pair distribution potentials.

The statistical mechanical model predictions replicate the MD simulations very well without any fitting parameters as shown in Figure 5-3. This example illustrates how difficult obtaining structural data from melt-quenched glasses can be. Additionally, it shows how the statistical mechanical model calculates structures in multi-component glasses by transferring interaction enthalpies from binary glasses. While the model prediction was convincing for MD simulated glasses, the uncertainty in the experimentally obtained data was too high to draw conclusions (Figure 5-1).

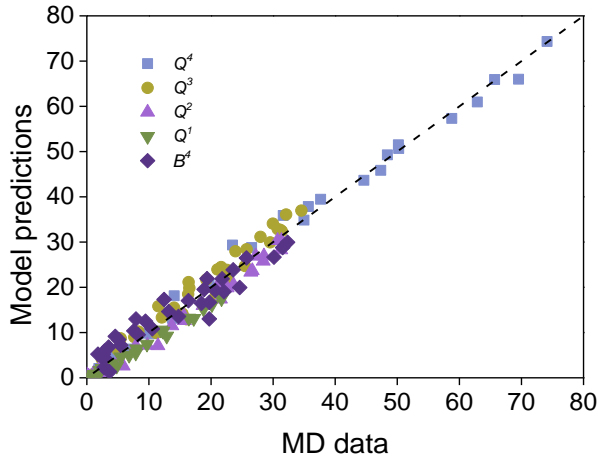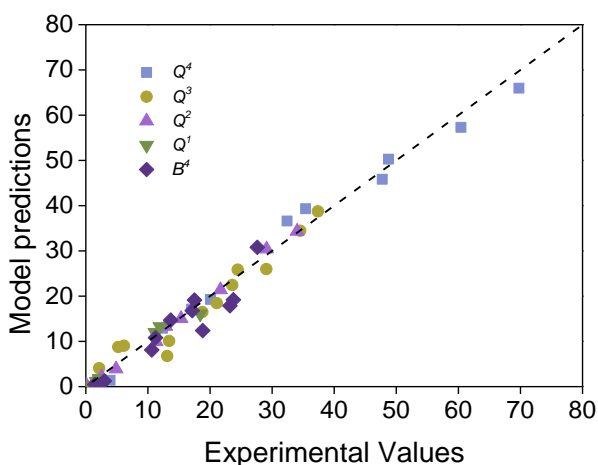*Figure 5-3. Structure data obtained by MD simulations in literature for potassium borosilicate glasses, compared to model predictions with 0 free parameters. The dashed line represents a one-to-one correlation. Reprinted from Paper C[28] under the Creative Commons Attribution License.*

5.2. STRUCTURE PREDICTION IN ALUMINOBORATE GLASSES

Aluminoborate glass is an intriguing glass family with a complex structure.[83,84] Aluminum is most commonly found in a 4-fold coordinated state with a negative charge stabilized by a modifier cation but may become 5-and 6-fold coordinated under certain conditions such as low alkali-containing glasses.[85] 5-and 6-fold coordinated aluminum ($Al^{5/6}$) acts as network modifiers to stabilize negatively charged former units or NBOs. Consequently, enthalpy values exist for each former-$Al^{5/6}$ interaction which must be established by fitting. Additionally, aluminum becomes 4-fold coordinated when interacting with another modifier ion:

$$Al^{5/6} + 2M_2O \rightarrow Al^4. \qquad (5\text{-}6)$$

In Figure 5-4, the Al-B interaction enthalpies have been obtained by fitting the model to experimentally obtained structural data (Paper I). All parameters used to obtain the fit presented in Figure 5-4 are reported in Table 5-2. As predicted in literature[39], sodium ions are (~11 times) more likely to interact with an $Al^{5/6}$ unit than a B^3 unit, which may lead to some interesting structural and physical responses as you increase the modifier content in an aluminoborate glass. Assuming the glass contains more aluminum than sodium, additional sodium ions will increase the network's connectivity by changing $Al^{5/6}$ to Al^4, but at the same time, reducing $Al^{5/6}$ will decrease the connectivity since B^4 units will return to B^3 units as the $Al^{5/6}$ species no longer stabilize them. With this model, the connectivity of the network may be predicted as a function of the composition
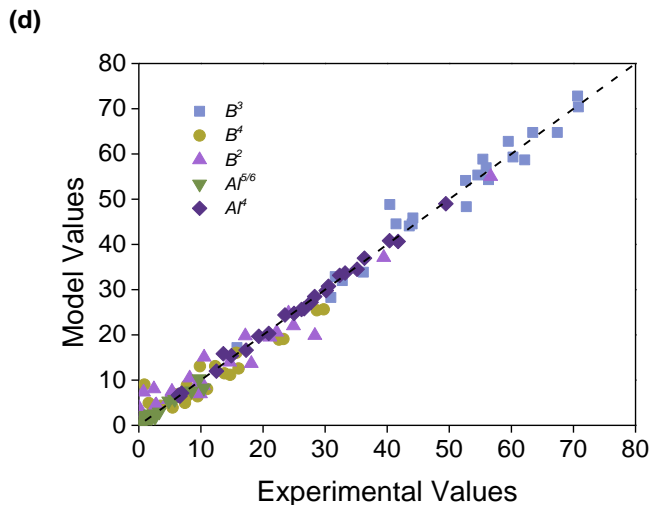
(d)

Figure 5-4. Na_2O-Al_2O_3-B_2O_3 structural data obtained by ^{27}Al and ^{11}B MAS NMR[refs] compared to model predictions. Al-B interactions fitted assuming $Al^{5/6}$ as modifying species, able to stabilize any negatively charged unit. Reprinted with permission from Paper I.

The parameters for Li^+ ions to interact with B^4 and B^2 units were determined using structural data from binary Li_2O-B_2O_3.[86] With these parameters established (Table 5-2), the model was fitted to experimentally obtained data for Li_2O-Al_2O_3-B_2O_3 glasses[84] (Figure 5-5) with only $w_{Al5/6}$ for Li^+ the free parameter. That the glass series fit very well with only one parameter supports the hypothesis of transferable parameters.

(a)
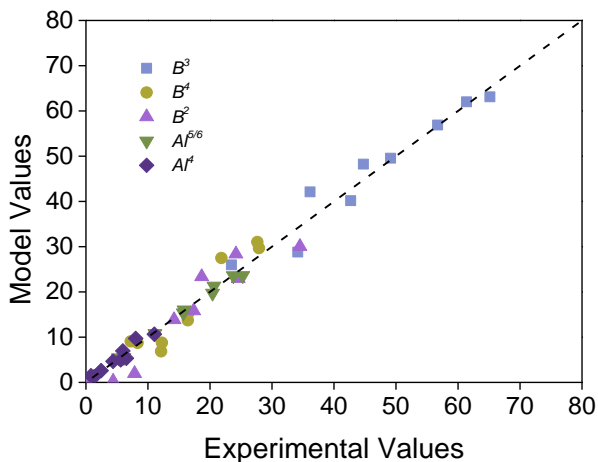
Figure 5-5. Li_2O-Al_2O_3-B_2O_3 structural data obtained by ^{27}Al and ^{11}B MAS NMR[Ref] compared to model predictions with only one free parameter. Reprinted with permission from Paper I.

The parameters in row 1 of Table 5-2 represent the weighting each possible $Al^{5/6}$ interaction has. These parameters provide insight into the structure in a theoretical binary Al_2O_3-B_2O_3 glass. An $Al^{5/6}$ unit is ~100 times more likely to interact with a B^3 to form and stabilize either a B^4 or a B^2 than to stabilize an Al^4 unit. With these parameters established, the structural units in a theoretical binary Al_2O_3-B_2O_3 glass may be described (Paper 1) as a function of [Al_2O_3] (Figure 5-6). Since binary Al_2O_3-B_2O_3 glasses are complicated to manufacture because they readily crystalize[87], this model provides valuable insight into the interactions between aluminum and boron species by extracting available experimental data from modified aluminoborate glasses.

Glass system	w_{B^3}	w_{B^4}	w_{B^2}	w_{B^1}	$w_{Al^{5/6}}$
Al^{3+}	1	0.071	0.065	0.031	0.011
Na^+	1	0.65	$1.4 \cdot 10^{-4}$	-	11.61
Li^+	1	0.19	0.58	-	4.14
Cs^+	1	1.37	$7.9 \cdot 10^{-10}$	-	30.69

Table 5-2. Relative Weighting factors (w_i), where i corresponds to a given structural configuration (B^3, B^4, B^2, B^1 and $Al^{5/6}$), for the fitting of the current statistical mechanical model to experimental structure data. The uncertainty of the weighting factor parameters is on the order of $\pm 5\%$. Reprinted with permission from Paper I.
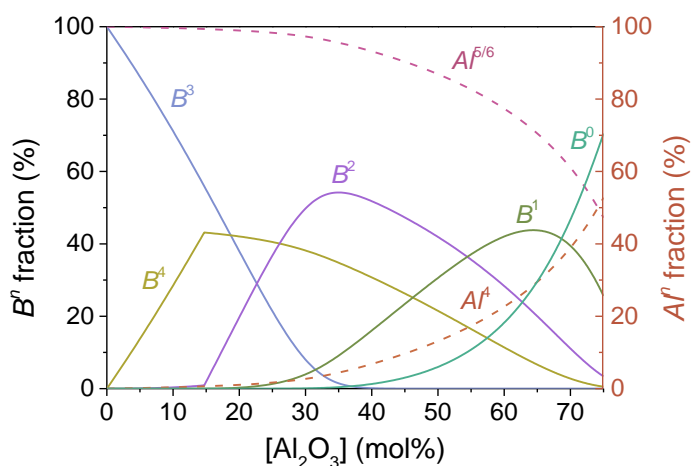
Figure 5-6. Model prediction of composition-structure relation in a binary Al_2O_3-B_2O_3 glass. Both Al^n and B^n fractions are relative to the total amount of Al_2O_3 and B_2O_3, respectively. Reprinted with permission from Paper I.

5.3. STRUCTURE PREDICTION IN PHOSPHOSILICATE GLASSES

The final mixed former system we will examine is the phosphosilicate system (Paper IV). Network modifiers typically break the glassy backbone by forming NBOs, however, Si^6 units formed in phosphosilicate glasses require network modifying cations to be charge-balanced (Figure 2-6).[46] Hence, the addition of network modifiers may either decrease the network connectivity by forming NBOs or increase the network connectivity by inducing the formation of Si^6 units. In Figure 5-7 (a), the modeling procedure explained for borosilicate glasses was used for Na_2O-SiO_2-P_2O_5 glasses. The enthalpy parameters used to obtain the model values in Figure 5-7 (a)

were obtained by fitting the statistical mechanics-based model to experimentally obtained structure data in the Na_2O-SiO_2 and Na_2O-P_2O_5 glass systems.[63,88,89] Figure 5-7 (a) shows that the model cannot capture the Si^6 units as these do not exist in the binary silicate glasses. An additional parameter (K_{Si6}) was included to account for Si^6 units in the phosphosilicate glasses in calculating the model results shown in Figure 5-7 (b). This parameter was included to account for the reaction between Si and P structure units to form Si^6 (Figure 2-6) and was derived from literature.[48]

$$\frac{[P^3]}{[SiO_2]} \cdot K_{Si^6} = \frac{[Si^6]}{[SiO_2]},\tag{5-7}$$

where $[SiO_2]$ is the total concentration of silica in the glass, and P^3 and Si^6 can be calculated iteratively, given that K_{Si6} is known.
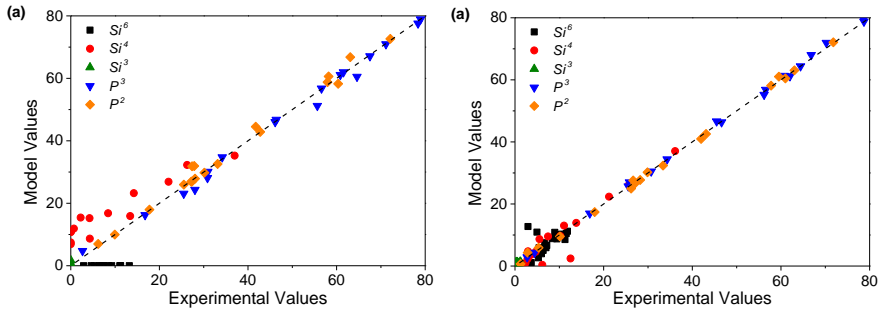
Figure 5-7. Comparison of model predictions and experimental data for the structural units in Na_2O-SiO_2-P_2O_5 (a) before and (b) after introducing Si^6 modeling for the structural units. The experimental data are from ^{29}Si and ^{31}P MAS NMR spectroscopy.[48,49,90] Reprinted with permission from Paper IV.

This example illustrates a case where the direct transfer of enthalpy values from binary to mixed-former glasses is insufficient for calculating the SRO structures. In this case, an additional parameter accounted for the additional complexity in the mixed-former glass. It is inefficient to account for the mixed-former effect on a per-system basis.

5.4. STATMECHGLASS: PYTHON-BASED MODELING SOFTWARE

A Python-based package was developed for easy use of the extensive statistical mechanical model StatMechGlass (Paper III). The package comes with already defined modifier-former interaction enthalpies and former-former interaction parameters and may be used to predict glass structures from compositions without any input files. In case the glass system of interest requires different interaction parameters, additional parameters can easily be input. The software has a feature for building the modifier-former interaction enthalpies from glass structure data input. Finally, the software can output composition-structure plots.

The software is implemented in the Python Packaging Index (PyPI), which is commonly recognized as the easiest way to install python packages directly to a script.

5.5. ACCOUNTING FOR MIXED-FORMER EFFECTS USING MACHINE LEARNING

As shown in the previous section, the statistical mechanical model does have a significant drawback of oversimplifying the mechanics governing the structure distribution in mixed-former glasses. While these errors could be corrected on a per-system basis, machine learning should quickly learn and correct for these systematic errors. It is the hypothesis that combining statistical mechanical modeling with machine learning could provide the extrapolative power of statistical mechanics and the precision of machine learning. Machine learning could indeed be used without statistical mechanics but requires a much larger dataset.[16,91] In Paper V, the idea is to teach the machine learning model the composition-structure relation captured by statistical mechanics to reduce the input-output complexity and hopefully getting a good fit with limited data. Optimally, the combined model can be used to predict structures of glass compositions in large composition-property databases even when trained on a relatively small dataset, hence allowing for large-scale composition-structure-property glass modeling. Machine learning models, and neural networks, in particular, have been successfully applied to glass systems to capture composition-property relations on a large scale for properties such as lattice thermal conductivity and glass-forming ability.[92,93] The composition-property relation in oxide glasses is often highly non-linear and complex, while the structure-property relation is much more linear. Combining statistical mechanics with machine learning could provide a suitable model for calculating structures of the property models' compositions, allowing for training on composition and structure. The composition-structure relation in glasses is also highly non-linear and complex, but most of the complexity is captured by statistical mechanics, which only leaves a small systematic error, which should be simple for machine learning to capture.

Multilayer perception neural network (MLP-NN) is a powerful machine learning model widely used for glass property prediction.[94-96] MLP-NN is made up of multiple layers of artificial neurons connected through artificial synapses. The input data is transformed by a given weight when transported through the synapse and transformed in the neuron by a non-linear activation function. When training, the model will optimize the weightings and the activation functions to best capture the output for the model. Other than the parameters optimized during training, the architecture of the neural network affects the predictive power. Here, both the number of neurons per layer and the number of layers affect the outcome and are traditionally referred to as hyperparameters. If the network is too simple for the dataset, the model will underfit, while a too complicated network architecture will overfit. The network architecture is adapted to give the best prediction of the current dataset (Paper V). To investigate the quality of prediction, a subset of the data is removed from the training data and used to validate the model.

Figures 5-8 (a), (b), and (c) show the prediction results from statistical mechanics, MLP-NN, and the combined model, respectively (Paper V). Statistical mechanics do slightly better when examining the root-mean-square errors (RMSE) than the composition-structure MLP-NN model. Additionally, the statistical mechanical model is trained on a smaller dataset relative to the validation set. The training sets are in specific glass systems, while the validation sets are entirely different, unlike the machine learning models, where the validation set is a random subset of the total data.
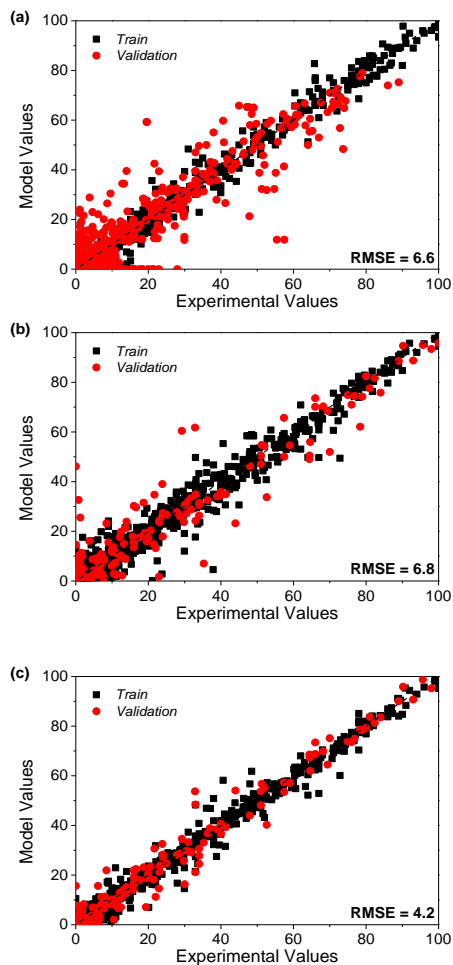
Figure 5-8. Experimentally obtained structural values plotted against the model predictions for training and validation sets. Black symbols refer to training data, while red symbols represent validation data. Model predictions are obtained using (a) statistical mechanics, (B) MLP-NN, and (c) a combination of statistical mechanics and MLP-NN. All experimentally obtained data from the literature. Reprinted from Paper V.

In summary, the statistical mechanical model better predicts a more extensive validation set with a smaller training set and with higher extrapolation than the MLP-NN model. When combining statistical mechanics with MLP-NN, the RMSE drops significantly. From this, it would seem that the MLP-NN model learns from the thermodynamic information indirectly supplied by the statistical mechanical approach without needing more raw data.

While it could be argued that the machine learning models learn the composition-structure relations themselves, this study has shown that the composition-structure relation is too non-linear for pure MLP-NN to learn with a limited dataset. Allowing the neural network to learn the thermodynamic contribution to the structure formation by supplying statistical mechanical structure results as an additional layer of input data allowed the model to predict the non-linear nature of composition-structure relations. This modeling approach could improve composition-property models' predictive and extrapolative power by offering the structural component and allowing for composition-structure-property modeling.

CHAPTER 6. CONCLUSIONS AND PERSPECTIVES

This thesis has highlighted examples of the application of statistical mechanics as a tool to predict the composition-property relation in oxide glasses by accounting for enthalpic and entropic contributions to SRO structure formation. In this chapter, the main findings are summarized, followed by a short discussion on the future implications of the work.

This study has focused on the statistical mechanical approach originally proposed by Mauro[51]. Throughout the project, the theoretical approach has been implemented, expanded, and verified in real glass systems. The adapted models were used to predict the distribution of structures in binary phosphate, silicate, and borate glasses with input from as little as two glasses. The model obtained relative enthalpies of structure formation from literature data of binary oxide glass structures. Additionally, it accounted for the thermal history of the glass by assuming a glassy structure similar to that of the glass-forming melt at the fictive temperature. The model can be used to capture the temperature dependence of structures in the glass-forming melt. The enthalpies combined with the thermal histories have shed light on the thermodynamical differences between different interactions occurring in the glass-forming melt. The statistical mechanical model also captured the mixed modifier anomaly, where structure correlates non-monotonically when mixing two or more modifiers. The combination of modifiers-former interaction competition and the effect of the thermal history explained this anomaly. These new understandings of glass structure may be helpful for future studies involved in those areas.

We have shown that the interaction enthalpies in binary silicate and borate glasses could be used directly to calculate the structures of borosilicate and aluminoborate glass systems with only one additional parameter for each former-former pair. By extending the model from binary glasses to multi-component glasses without additional parameters, the potential output of the model scales exponentially as the input scales linearly. This is especially useful as experimentally obtaining good-quality structure data becomes increasingly difficult the more components are introduced in the glasses. The statistical mechanical model can be applied in the future to predict structures of glasses with too many components to obtain reliable structure data. However, for phosphosilicate glasses, this approach was insufficient as former-former interactions occurred between Si and P, requiring one more parameter to capture the structures. The open-source StatMechGlass software was built to easily apply the statistical mechanical model in both binary and multi-component glasses. This software offers precise structure prediction in the glass systems presented in this thesis and can easily be extended beyond those systems but should be verified against experimental structure data. The software allows for easy use of the pretty complex

models described in this thesis. As the model has been tailored to each glass system, it would be difficult to replicate the results without a tool like StatMechGlass. This allows for this work to be expanded upon without too much difficulty.

Finally, the statistical mechanical model trained on binary data was used in combination with machine learning to very precisely predict the structures of multi-component glasses. By combining statistical mechanics with machine learning, the model captures the thermodynamics of structure formation while also capturing errors such as the Si-P interaction mentioned above. The combination of the two powerful modeling techniques outperformed either technique when used alone. The combined model also showed excellent extrapolation and precisely predicted the structure of glasses outside the composition of the training data.

The novel machine learning model was also translated to python code available for all researchers to make their structure predictions. With this code, structures can be predicted for an extensive range of glass compositions. It could be beneficial for property predicting models based on large datasets with glass compositions and their resulting properties to implement this new model. The new model could provide structure data for a significant fraction of the compositions of the original dataset. Thus, both composition and structure could be input parameters for the property model. Since structure has been shown to correlate better with properties than composition, the knowledge of the glassy structures may offer better property prediction.

LITERATURE LIST

[1] S.C. Rasmussen, Origins of Glass: Myth and Known History, in: Anonymous How Glass Changed the World, Springer Berlin Heidelberg, Berlin, Heidelberg, 2012, pp. 11-19.

[2] D.E. Day, Mixed alkali glasses - Their properties and uses, Journal of Non-Crystalline Solids. 21 (1976) 343-372.

[3] J. Phillips, R. Kerner, Structure and function of window glass and Pyrex, The Journal of Chemical Physics. 128 (2008) 174506-174506.

[4] A.N.Z. Rashed, Mohamed, Abd El-Naser Abd El Gawad, Hanafy, Sakr Abd El Rahim Salman, M.H. Aly, A comparative study of the performance of graded index perfluorinated plastic and alumino silicate optical fibers in internal optical interconnections, Optik. 127 (2016) 9259-9263.

[5] T. Miyashita, T. Manabe, Infrared Optical Fibers, IEEE Transactions on Microwave Theory and Techniques. 30 (1982) 1420-1438.

[6] M.J. Plodinec, Borosilicate glasses for nuclear waste imobilisation, Glass Technology. 41 (2000) 186.

[7] D.E. Day, Z. Wu, C.S. Ray, P. Hrma, Chemically durable iron phosphate glass wasteforms, Journal of Non-Crystalline Solids. 241 (1998) 1-12.

[8] M.N. Rahaman, D.E. Day, B. Sonny Bal, Q. Fu, S.B. Jung, L.F. Bonewald, A.P. Tomsia, Bioactive glass in tissue engineering, Acta Biomaterialia. 7 (2011) 2355-2373.

[9] J.R. Jones, Review of bioactive glass: From Hench to hybrids, Acta Biomaterialia. 9 (2013) 4457-4486.

[10] J.C. Mauro, C.S. Philip, D.J. Vaughn, M.S. Pambianchi, Glass Science in the United States: Current Status and Future Directions, International Journal of Applied Glass Science. 5 (2014) 2-15.

[11] S. Baghel, H. Cathcart, N.J. O'Reilly, Polymeric Amorphous Solid Dispersions: A Review of Amorphization, Crystallization, Stabilization, Solid-State Characterization, and Aqueous Solubilization of Biopharmaceutical Classification System Class II Drugs, Journal of Pharmaceutical Sciences. 105 (2016) 2527-2544.

[12] E. Axinte, Glasses as engineering materials: A review, Materials & Design. 32 (2011) 1717-1732.

[13] E.D. Zanotto, F.A.B. Coutinho, How many non-crystalline solids can be made from all the elements of the periodic table? Journal of Non-Crystalline Solids. 347 (2004) 285-288.

[14] J.C. Mauro, Grand Challenges in Glass Science, Frontiers in Materials. 1 (2014) 1-20.

[15] J.C. Mauro, A. Tandia, K.D. Vargheese, Y.Z. Mauro, M.M. Smedskjaer, Accelerating the Design of Functional Glasses through Modeling, Chemistry of Materials. 28 (2016) 4267-4277.

[16] H. Liu, Z. Fu, K. Yang, X. Xu, M. Bauchy, Machine learning for glass science and engineering: A review, Journal of Non-Crystalline Solids. 557 (2021) 119419.

[17] M.M. Smedskjaer, J.C. Mauro, S. Sen, Y. Yue, Quantitative Design of Glassy Materials Using Temperature-Dependent Constraint Theory, Chemistry of Materials. 22 (2010) 5358-5365.

[18] G. Carleo, I. Cirac, K. Cranmer, L. Daudet, M. Schuld, N. Tishby, L. Vogt-Maranto, L. Zdeborová, Machine learning and the physical sciences, Rev. Mod. Phys. 91 (2019) 045002.

[19] H. Liu, Z. Fu, K. Yang, X. Xu, M. Bauchy, Machine learning for glass science and engineering: A review, Journal of Non-Crystalline Solids. 557 (2021) 119419.

[20] Q. Tong, P. Gao, H. Liu, Y. Xie, J. Lv, Y. Wang, J. Zhao, Combining Machine Learning Potential and Structure Prediction for Accelerated Materials Design and Discovery, J. Phys. Chem. Lett. 11 (2020) 8710-8720.

[21] M. Bauchy, Deciphering the atomic genome of glasses by topological constraint theory and molecular dynamics: A review, Computational Materials Science. 159 (2019) 95-102.

[22] J.C. Mauro, Topological constraint theory of glass, American Ceramic Society Bulletin. 90 (2011) 31-37.

[23] M.M. Smedskjaer, C. Hermansen, R.E. Youngman, Topological engineering of glasses using temperature-dependent constraints, MRS bulletin. 42 (2017) 29-33.

[24] A. Flambarda, L. Montagnea, L. Delevoyea, G. Palavita, J.P. Amoureuxa, J.J. Videaub, Solid-state NMR study of mixed network sodium–niobium phosphate glasses, Journal of Non-Crystalline Solids. 345-346 (2004) 75-79.

[25] R. Youngman, NMR Spectroscopy in Glass Science: A Review of the Elements, Materials. 11 (2018) 476.

[26] M.S. Bødker, J.C. Mauro, S. Goyal, R.E. Youngman, M.M. Smedskjaer, Predicting Q-Speciation in Binary Phosphate Glasses Using Statistical Mechanics, The Journal of Physical Chemistry. B.. 122 (2018) 7609.

[27] M.S. Bødker, J.C. Mauro, R.E. Youngman, M.M. Smedskjaer, Statistical Mechanical Modeling of Borate Glass Structure and Topology: Prediction of Superstructural Units and Glass Transition Temperature, The Journal of Physical Chemistry. B. 123 (2019) 1206-1213.

[28] M.S. Bødker, S.S. Sørensen, J.C. Mauro, M.M. Smedskjaer, Predicting Composition-Structure Relations in Alkali Borosilicate Glasses Using Statistical Mechanics, Frontiers in Materials. 6 (2019).

[29] J. Shelby, Introduction to Glass Science and Technology, 2nd ed., Royal Society of Chemistry, 2005.

[30] A. Varschneya, J. Mauro, Fundamentals of Inorganic Glasses, 3rd ed., Elsevier, 2019.

[31] X. Li, W. Song, K. Yang, N.M.A. Krishnan, B. Wang, M.M. Smedskjaer, J.C. Mauro, G. Sant, M. Balonis, M. Bauchy, X. Li, W. Song, K. Yang, N.M.A. Krishnan, B. Wang, M.M. Smedskjaer, J.C. Mauro, G. Sant, M. Balonis, M. Bauchy, Cooling rate effects in sodium silicate glasses: Bridging the gap between molecular dynamics simulations and experiments, The Journal of Chemical Physics. 147 (2017).

[32] Q. Zheng, Y. Zhang, M. Montazerian, O. Gulbiten, J.C. Mauro, E.D. Zanotto, Y. Yue, Understanding Glass through Differential Scanning Calorimetry, Chem. Rev. 119 (2019) 7848.

[33] N. Deopa, A.S. Rao, Spectroscopic studies of Sm^{3+} ions activated lithium lead alumino borate glasses for visible luminescent device applications, Optical materials. 72 (2017) 31.

[34] F. Almutawa, R. Vandal, S.Q. Wang, H.W. Lim, Current status of photoprotection by window glass, automobile glass, window films, and sunglasses, Photodermatology, Photoimmunology & Photomedicine. 29 (2013) 65-72.

[35] K.C. Lyon, Prediction of the viscosities of soda-lime silica glasses, Journal of research of the National Bureau of Standards. Section A. Physics and Chemistry. 78A (1974) 497-504.

[36] J.F. Emerson, P.E. Stallworth, P.J. Bray, High-field ^{29}Si NMR studies of alkali silicate glasses, Journal of Non-Crystalline Solids. 113 (1989) 253-259.

[37] W. Hater, W. Müller-Warmuth, M. Meier, G.H. Frischat, High-resolution solid-state NMR studies of mixed-alkali silicate glasses, Journal of Non-Crystalline Solids. 113 (1989) 210-212.

[38] R.E. Youngman, S.T. Haubrich, J.W. Zwanziger, M.T. Janicke, B.F. Chmelka, Short-and Intermediate-Range Structural Ordering in Glassy Boron Oxide, Science. 269 (1995) 1416-1420.

[39] M. Bertmer, L. Züchner, J.C.C. Chan, H. Eckert, Short and Medium Range Order in Sodium Aluminoborate Glasses. 2. Site Connectivities and Cation Distributions Studied by Rotational Echo Double Resonance NMR Spectroscopy, The Journal of Physical Chemistry. B. 104 (2000) 6541-6553.

[40] D.C. Kaseman, A. Retsinas, A.G. Kalampounias, G.N. Papatheodorou, S. Sen, Q-Speciation and Network Structure Evolution in Invert Calcium Silicate Glasses, The Journal of Physical Chemistry. B. 119 (2015) 8440-8445.

[41] M.M. Lima, R. Monteiro, Characterisation and thermal behaviour of a borosilicate glass, Thermochimica Acta. 373 (2001) 69-74.

[42] M. Bengisu, M. Bengisu, Borate glasses for scientific and industrial applications: a review, J Mater Sci. 51 (2016) 2199-2242.

[43] J. Zhong, P.J. Bray, Boron coordination by NMR - mixed alkali effect, Journal of Non-Crystalline Solids. 111 (1989) 67.

[44] R.K. Brow, Review: the structure of simple phosphate glasses, Journal of Non-Crystalline Solids. 263-264 (2000) 1-28.

[45] R.K. Brow, R.J. Kirkpatrick, G.L. Turner, The short range structure of sodium phosphate glasses I. MAS NMR studies, Journal of Non-Crystalline solids. 116 (1990) 39-45.

[46] H. Yamashita, H. Yoshino, K. Nagata, I. Yamaguchi, M. Ookawa, T. Maekawa, NMR and Raman studies of Na_2O-P_2O_5-SiO_2 glasses - Six-coordinated Si and basicity, Journal of Ceramic Society Japan. 106 (1998) 539-544.

[47] H. Yamashita, H. Yoshino, K. Nagata, H. Inoue, T. Nakajin, T. Maekawa, Nuclear magnetic resonance studies of alkaline earth phosphosilicate and aluminoborosilicate glasses, Journal of Non-Crystalline Solids. 270 (2000) 48-59.

[48] J. Ren, H. Eckert, Superstructural Units Involving Six-Coordinated Silicon in Sodium Phosphosilicate Glasses Detected by Solid-State NMR Spectroscopy, J. Phys. Chem. C. 122 (2018) 27620.

[49] D. Miyabe, M. Takahashi, Y. Tokuda, T. Yoko, T. Uchino, Structure and formation mechanism of six-fold coordinated silicon in phosphosilicate glasses, Phys. Rev. B. 71 (2005) 172202.

[50] H. Zeng, Q. Jiang, Z. Liu, X. Li, J. Ren, G. Chen, F. Liu, S. Peng, Unique Sodium Phosphosilicate Glasses Designed Through Extended Topological Constraint Theory, The Journal of Physical Chemistry. B. 118 (2014) 5177-5183.

[51] J.C. Mauro, Statistics of modifier distributions in mixed network glasses, The Journal of Chemical Physics. 138 (2013) 12A522.

[52] J.C. Mauro, M.M. Smedskjaer, Statistical mechanics of glass, Journal of Non-Crystalline Solids. 396-397 (2014) 41-53.

[53] A. Fog, Sampling Methods for Wallenius' and Fisher's Noncentral Hypergeometric Distributions, Communications in Statistics - Simulation and Computation. 37 (2008) 241-257.

[54] J. S. Rowlinson, The Maxwell–Boltzmann distribution, Molecular Physics. 103 (2005) 2821-2828.

[55] S. Goyal, J.C. Mauro, Statistical mechanical model of bonding in mixed modifier glasses, Journal of the American Ceramic Society. 101 (2018) 1906-1915.

[56] K.A. Kirchner, S.H. Kim, J.C. Mauro, Statistical mechanics of topological fluctuations in glass-forming liquids, Physica A. 510 (2018) 787-801.

[57] K.A. Kirchner, M.S. Bødker, M.M. Smedskjaer, S.H. Kim, J.C. Mauro, Statistical Mechanical Model of Topological Fluctuations and the Intermediate Phase in Binary Phosphate Glasses, The Journal of Physical Chemistry. B. 123 (2019) 7640-7648.

[58] K.A. Kirchner, J.C. Mauro, Statistical mechanical model of the self-organized intermediate phase in glass-forming systems with adaptable network topologies, Frontiers in materials. 6 (2019).

[59] A. Mandlule, F. Döhler, L. van Wüllen, T. Kasuga, D.S. Brauer, Changes in structure and thermal properties with phosphate content of ternary calcium sodium phosphate glasses, Journal of Non-Crystalline Solids. 392-393 (2014) 31-38.

[60] H. Eckert, Spying with spins on messy materials: 60 Years of glass structure elucidation by NMR spectroscopy, Int J Appl Glass Sci. 9 (2018) 167.

[61] L. van Wüllen, H. Eckert, G. Schwering, Structure−Property Correlations in Lithium Phosphate Glasses: New Insights from ^{31}P ↔ ^{7}Li Double-Resonance NMR, Chemistry of Materials. 12 (2000) 1840-1846.

[62] T.M. Alam, R.K. Brow, Local structure and connectivity in lithium phosphate glasses: a solid-state alp MAS NMR and 2D exchange investigation, Journal of Non-Crystalline Solids. 223 (1998) 1.

[63] H. Maekawa, T. Maekawa, K. Kawamura, T. Yokokawa, The structural groups of alkali silicate glasses determined from ^{29}Si MAS-NMR, Journal of Non-Crystalline Solids. 127 (1991) 53-64.

[64] J. Du, A.N. Cormack, The medium range structure of sodium silicate glasses: a molecular dynamics simulation, Journal of Non-Crystalline Solids. 349 (2004) 66-79.

[65] A.N. Cormack, Y. Cao, Molecular Dynamics Simulation of Silicate Glasses, Molecular Engineering. 6 (1996) 183-227

[66] L. Adkins, A. Cormack, Large-scale simulations of sodium silicate glasses, Journal of Non-Crystalline Solids. 357 (2011) 2538-2541.

[67] J. Kjeldsen, M.M. Smedskjaer, J.C. Mauro, Y. Yue, On the origin of the mixed alkali effect on indentation in silicate glasses, Journal of Non-Crystalline Solids. 406 (2014) 22-26.

[68] C. Calahoo, J.W. Zwanziger, The mixed modifier effect in ionic conductivity and mechanical properties for xMgO-(50-x)CaO-50SiO$_2$ glasses, Journal of Non-Crystalline Solids. 460 (2017) 6-18.

[69] T. Nanba, M. Nishimura, Y. Miura, A theoretical interpretation of the chemical shift of ^{29}Si NMR peaks in alkali borosilicate glasses, Geochimica et Cosmochimica acta. 68 (2004) 5103-5111.

[70] M. Wang, N.M. Anoop Krishnan, B. Wang, M.M. Smedskjaer, J.C. Mauro, M. Bauchy, A new transferable interatomic potential for molecular dynamics simulations of borosilicate glasses, Journal of Non-Crystalline Solids. 498 (2018) 294-304.

[71] L. Du, J.F. Stebbins, Nature of Silicon−Boron Mixing in Sodium Borosilicate Glasses: A High-Resolution ^{11}B and ^{17}O NMR Study, The Journal of Physical Chemistry. B. 107 (2003) 10063-10076.

[72] E.V. Belova, Y.A. Kolyagin, I.A. Uspenskaya, Structure and glass transition temperature of sodium-silicate glasses doped with iron, Journal of Non-Crystalline Solids. 423-424 (2015) 50-57.

[73] J. Zhong, P.J. Bray, Change in Boron Coordination in Alkali Borate Glasses, and Mixed Alkali Effects, as Elucidated by NMR, Journal of Non-Crystalline Solids. 111 (1989) 67.

[74] J.E. Shelby, Thermal Expansion of Alkali Borate Glasses, Journal of the American Ceramic Society. 66 (1983) 225-227.

[75] L. van Wüllen, W. Müller-Warmuth, D. Papageorgiou, H.J. Pentinghaus, Characterization and structural developments of gel-derived borosilicate glasses: a multinuclear MAS-NMR study, Journal of Non-Crystalline Solids. 171 (1994) 53-67.

[76] F. Angeli, O. Villain, S. Schuller, T. Charpentier, D. de Ligny, L. Bressel, L. Wondraczek, Effect of Temperature and Thermal History on Borosilicate Glass Structure, Physical review. B, Condensed Matter and Materials Physics. 85 (2012).

[77] A. Grandjean, M. Malki, V. Montouillout, F. Debruycker, D. Massiot, Electrical conductivity and ^{11}B NMR studies of sodium borosilicate glasses, Journal of Non-Crystalline Solids. 354 (2008) 1664-1670.

[78] L. Deng, J. Du, Development of boron oxide potentials for computer simulations of multicomponent oxide glasses, Journal of the American Ceramic Society. 102 (2018) 1.

[79] J.F. Stebbins, Anionic speciation in sodium and potassium silicate glasses near the metasilicate ($[Na,K]_2SiO_3$) composition: ^{29}Si, ^{17}O, and ^{23}Na MAS NMR, Journal of Non-Crystalline Solids: X. 6 (2020) 100049.

[80] W.M. Macdonald, A.C. Anderson, J. Schroeder, Low-temperature behavior of potassium and sodium silicate glasses, Physical Review. B, Condensed Matter. 31 (1985) 1090-1101.

[81] C.M. Kuppinger, J.E. Shelby, Viscosity and Thermal Expansion of Mixed-Alkali Sodium-Potassium Borate Glasses, Journal of the American Ceramic Society. 68 (1985) 463-467.

[82] R.E. Youngman, J.W. Zwanziger, Network Modification in Potassium Borate Glasses: Structural Studies with NMR and Raman Spectroscopies, Journal of Physical Chemistry 100 (1996) 16720-16728.

[83] S. Kapoor, R.E. Youngman, K. Zakharchuk, A. Yaremchenko, N.J. Smith, A. Goel, Structural and Chemical Approach toward Understanding the Aqueous Corrosion of Sodium Aluminoborate Glasses, The Journal of Physical Chemistry. B. 122 (2018) 10913-10927.

[84] H.R. Fernandes, S. Kapoor, Y. Patel, K. Ngai, K. Levin, Y. Germanov, L. Krishtopa, S. Kroeker, A. Goel, Composition-structure-property relationships in Li_2O–Al_2O_3–B_2O_3 glasses, Journal of Non-Crystalline Solids. 502 (2018) 142-151.

[85] K. Januchta, R.E. Youngman, A. Goel, M. Bauchy, S.L. Logunov, S.J. Rzoska, M. Bockowski, L.R. Jensen, M.M. Smedskjaer, Discovery of Ultra-Crack-Resistant Oxide Glasses with Adaptive Networks, Chem. Mater. 29 (2017) 5865.

[86] Y.H. Yun, P.J. Bray, Nuclear Magnetic Resonance Studies of Li_2O-B_2O_3 Glasses of High Li_2O Content, Journal of Non-Crystalline Solids. 44 (1981) 227.

[87] T. Yang, A. Bartoszewicz, J. Ju, J. Sun, Z. Liu, X. Zou, Y. Wang, G. Li, F. Liao, B. Martín-Matute, J. Lin, Microporous Aluminoborates with Large Channels: Structural and Catalytic Properties, Angewandte Chemie International Edition. 50 (2011) 12555-12558.

[88] S. Prabakar, R.M. Wenslow, K.T. Mueller, Structural properties of sodium phosphate glasses from $^{23}Na \rightarrow {}^{31}P$ cross-polarization NMR, Journal of Non-Crystalline Solids. 263-264 (2000) 82-93.

[89] W. Strojek, H. Eckert, Medium-range order in sodium phosphate glasses: A quantitative rotational echo double resonance solid state NMR study, Physical Chemistry Chemical Physics. 8 (2006) 2276-2285.

[90] C. Hermansen, X. Guo, R.E. Youngman, J.C. Mauro, M.M. Smedskjaer, Y. Yue, Structure-topology-property correlations of sodium phosphosilicate glasses, J. Chem. Phys. 143 (2015) 064510.

[91] G. Carleo, I. Cirac, K. Cranmer, L. Daudet, M. Schuld, N. Tishby, L. Vogt-Maranto, L. Zdeborová, Machine learning and the physical sciences, Rev. Mod. Phys. 91 (2019) 045002.

[92] Y.T. Sun, H.Y. Bai, M.Z. Li, W.H. Wang, Machine Learning Approach for Prediction and Understanding of Glass-Forming Ability, J. Phys. Chem. Lett. 8 (2017) 3434-3439.

[93] L. Chen, H. Tran, R. Batra, C. Kim, R. Ramprasad, Machine learning models for the lattice thermal conductivity prediction of inorganic materials, Computational Materials Science. 170 (2019) 109155.

[94] B. Cheng, D.M. Titterington, Neural Networks: A Review from a Statistical Perspective, Statistical Science. 9 (1994) 2-30.

[95] S. Bishnoi, S. Singh, R. Ravinder, M. Bauchy, N.N. Gosvami, H. Kodamana, N.M.A. Krishnan, Predicting Young's modulus of oxide glasses with sparse datasets using machine learning, Journal of Non-Crystalline Solids. 524 (2019) 119643.

[96] D.R. Cassar, A. Carvalho, E.D. Zanotto, Predicting glass transition temperatures using neural networks, Acta Materialia. 159 (2018) 249-256.